A Blind Source Separation Technique for Document Restoration Based on Edge Estimation

Antonio Boccuto   Ivan Gerace   Valentina Giorgetti
Gabriele Valenti *

Abstract

In this paper we study a *Blind Source Separation* (BSS) problem, and in particular we deal with document restoration. We consider the classical linear model. To this aim, we analyze the derivatives of the images instead of the intensity levels. Thus, we can establish a non-overlapping constraints on document sources. Moreover, we impose that the rows of the mixture matrices of the sources have sum equal to 1, in order to keep equal the lightnesses of the estimated sources and of the data. Here we give a technique which uses the symmetric factorization, whose goodness is tested by the experimental results.

1 Introduction

In this paper we deal with a *Blind Source Separation* (BSS) problem. This problem has been an active research topic in signal processing since the end of the last century, and has several applications in different fields. Here we deal with *show-through* and *bleed-through* effects. The show-through is a front-to-back interference, mainly due to the scanning process and the

*Dipartimento di Matematica e Informatica, Università di Perugia, via Vanvitelli 1, I-06123 Perugia, Italy, Dipartimento di Matematica e Informatica, Università di Firenze, viale G. B. Morgagni 67/A, I-50134 Firenze; e-mail: antonio.boccuto@unipg.it, ivan.gerace@unipg.it, valentina.giorgetti@unifi.it, gabriele.valenti87@gmail.com
Keywords:
2010 A. M. S. Subject Classifications: Primary: 68R15. Secondary: 05A05, 68R05.

transparency of the paper, which causes the text in the verso side of the document to appear also in the recto side (and vice versa). The bleed-through is an intrinsic front-to-back physical deterioration due to ink seeping, and produces an effect similar to that of show-through.

We consider a classical linear and stationary recto-verso model (see also [4, 9, 10, 11, 17]) developed for this purpose, and we deal with the problem of estimating both the ideal source images of the recto and the verso of the document and the mixture matrix producing the bleed-through or show-through effects. This problem is ill-posed in the sense of Hadamard (see also [8]). In fact, since the estimated mixture matrix varies, the corresponding estimated sources are in general different, and thus we have infinitely many solutions. Many techniques to solve this problem have been proposed in the literature. Among them, the *Independent Component Analysis* (ICA) methods are based on the assumption that the sources are mutually independent (see also [6]). The best-known ICA technique is the so-called FastICA (see also [9, 10, 11, 12, 13]), which finds an orthogonal rotation of the prewhitened data which maximizes a measure of non-Gaussianity of the rotated components, using a fixed point iteration. The FastICA algorithm is a parameter-free and extremely fast procedure, but ICA is not a suitable approach in our setting, as for the problem we consider there is a clear correlation among the sources. On the other hand, several techniques for ill-posed inverse problems require that the estimated sources are only mutually uncorrelated. In this case, they are determined by a linear transformation of the data, which is obtained by imposing either an orthogonality condition, as in *Principal Component Analysis* (PCA) (see also [4, 16, 17]), or an orthonormality condition, as in *Whitening* (W) and *Symmetric Whitening* (SW) techniques (see also [4, 16, 17]). These approaches require only a unique and very fast processing step. In [4, 17] it is observed that the results obtained by the SW method are substantially equivalent to those given by an ICA technique in the symmetric mixing case.

In [2] it is assumed that the sum of all rows of the mixing matrix is equal to one, since we expect that the color of the background of the source is the same as that of the data. In [2] a change of variables concerning the data is made so that high and low light intensities correspond to presence and absence of text in the document, respectively, and we impose a nonnegativity constraint on the estimated sources (see also [3, 5, 7, 14]). In [2] the *overlapping matrix* of both the observed data and the ideal sources is defined, namely a quantity related to the cross-correlation between the signals. From the overlapping matrix it is possible to deduce the *overlapping level*, which measures the similarity between the front and the back of the document. In this paper we modify the technique proposed in [2] and we deal with the derivatives of the images of the original sources. In this case, we assume that the overlapping level is equal to zero. By means of our experimental results, we show that the proposed technique improves the results obtained in [2] in terms both of accuracy of the estimates and of computational costs. We refer to this method as the *Zero Edge Overlapping in Document Separation* (ZEODS) algorithm.

In Section 2 we present the linear model. In Section 3 we develop the ZEODS algorithm to deal with the linear problem. In Section 4 we compare experimentally the ZEODS algorithm with other fast and unsupervised methods existing in the literature.

2 The linear model

The classical linear model is the following (see, e.g., [4, 9, 10, 11, 15, 17]):

$$\widehat{x}^T = A\,\widehat{s}^T, \tag{1}$$

where $\cdot^T$ is the transpose operator of a matrix, $\widehat{x} \in [0, 255]^{nm}$ is the *data document* in the involved subdomain, $\widehat{s} \in [0, 255]^{nm}$ is the *source document*, n (resp., m) is the number of rows (resp., columns) of the considered images, and $A \in \mathbb{R}^{2\times 2}$ is the *mixture matrix*.

In this paper we discuss the problem of evaluating the ideal sources and the mixture matrix from the observed data using the linear equation (1), which is a *Blind Source Separation* (BSS) problem (see, e.g., [4, 16]). If we get an invertible estimate $\widetilde{A}$ of A, then an estimate of s is given by

$$\widetilde{s}^T = \widetilde{A}^{-1}\widehat{x}^T. \tag{2}$$

Since there are infinitely many choices of $\widetilde{A}$, our problem admits infinitely many solutions, and is ill-posed in the sense of Hadamard. Also when $\widetilde{A}$ and $\widetilde{s}$ are nonnegative matrices, the problem is NP-hard (see [18]) and ill-posed (see [8]). To overcome this, we impose some constraints on the solutions.

We do not assume that the mixing matrix is symmetric, because the phenomenon of infiltration of the ink is often unpredictable. However, since the color of the paper is the same for each part of the document, we suppose that the value of the source background, that is the graylevel of the unprinted/unwritten paper, is the same as the background of the data. This value corresponds to the light intensity of the paper on which the document is written. To impose this condition, we require that A is a *one row-sum matrix*, namely

$$a_{11} + a_{12} = a_{21} + a_{22} = 1. \tag{3}$$

We call *clique* the set of pixels on which the finite difference of first order is well-defined. The vertical cliques are of the type

$$c = \{(i, j), (i + 1, j)\}, \tag{4}$$

while the horizontal cliques have the form

$$c = \{(i, j), (i, j + 1)\}. \tag{5}$$

We denote by C the set of all cliques. Note that $|C| = 2nm - m - n$, where C denotes the cardinality of C.

Given a vertical clique $c = \{(i, j), (i + 1, j)\}$, the finite difference operator on it is $\Delta_c \widehat{\mathbf{x}} = \widehat{x}_{i,j} - \widehat{x}_{i+1,j}$. Moreover, given a horizontal clique $c = \{(i, j), (i, j + 1)\}$, the associated finite difference operator is let $\Delta_c \widehat{\mathbf{x}} = \widehat{x}_{i,j} - \widehat{x}_{i,j+1}$. We consider the linear operator $D \in \mathbb{R}^{|C| \times nm}$. Note that, in this matrix, every row index corresponds to a clique, while every column index corresponds to a pixel. To every row it is possible to associate a vertical or horizontal clique. Then, if we consider a vertical clique $c = \{(i, j), (i + 1, j)\}$, we get

$$D_{c,(l,k)} = \begin{cases} 1, & \text{if } (l, k) = (i, j), \\ \\ -1, & \text{if } (l, k) = (i + 1, j), \\ \\ 0, & \text{otherwise;} \end{cases}$$

and, if $c = \{(i, j), (i, j + 1)\}$ is a horizontal clique, we have

$$D_{c,(l,k)} = \begin{cases} 1, & \text{if } (l, k) = (i, j), \\ \\ -1, & \text{if } (l, k) = (i, j + 1), \\ \\ 0, & \text{otherwise.} \end{cases}$$

Let $x \in \mathbb{R}^{|C| \times 2}$ be the *data derivative document matrix* defined by

$$x = D\widehat{x}. \tag{6}$$

Analogously, the *source derivative matrix* $s \in \mathbb{R}^{|C| \times 2}$ is defined by

$$s = D\widehat{s}. \tag{7}$$

Notice that the involved images contain letters. If we assume that the colours of the letters and of the background are uniform, then the finite differences are null, while they are different from zero in correspondence with the edges of the letters.

From (1), (6) and (7) we deduce

$$x^T = \widehat{x}^T D^T = A\widehat{s}^T D^T = As^T. \tag{8}$$

Note that the linear model obtained by considering the data document derivative matrix and the source derivative matrix is equal to that obtained by treating the data document and the source document in (1).

Analogously as in [2], here we define the following 2×2 *data derivative overlapping matrix* of the observed data:

$$C = \begin{bmatrix} c_{11} & c_{12} \\ c_{21} & c_{22} \end{bmatrix} = x^T x = \begin{bmatrix} x_r^T \cdot x_r & x_r^T \cdot x_v \\ x_v^T \cdot x_r & x_v^T \cdot x_v \end{bmatrix}. \tag{9}$$

The matrix C indicates how much the edges of the letters in the front overlap with those of the back. Indeed, in our case, the data derivative overlapping matrix is always nonnegative, and is diagonal if and only if there is no overlapping of the edges of text from the recto to the verso of the document. In particular we refer to the entries $d = c_{12} = c_{21}$ as the *data derivative overlapping level.*

The *source derivative overlapping matrix* can be defined similarly as

$$P = \begin{bmatrix} p_{11} & p_{12} \\ p_{21} & p_{22} \end{bmatrix} = s^T s = \begin{bmatrix} s_r^T \cdot s_r & s_r^T \cdot s_v \\ s_v^T \cdot s_r & s_v^T \cdot s_v \end{bmatrix}.$$

It is not difficult to see that the matrices C and P are symmetric and positive semidefinite. We refer to the value

$$k = p_{12} = p_{21} = s_r^T \cdot s_v \tag{10}$$

as the *source derivative overlapping level.* We assume that $k = 0$, that is the edges of the recto of the document do not overlap with those of the verso.

3 A technique for solving the linear problem

As in [2], we define a *symmetric factorization* of a symmetric and positive-definite matrix $H \in \mathbb{R}^{n \times n}$ as an expression of the type $H = ZZ^T$, where $Z \in \mathbb{R}^{n \times n}$. Note that, given an orthogonal matrix $Q \in \mathbb{R}^{n \times n}$ and a symmetric factorization of the type $H = ZZ^T$, then $ZQ(ZQ)^T$ is a symmetric factorization of H too. Furthermore, if we pick any two symmetric factorizations $H = Z_1 Z_1^T$ and $H = Z_2 Z_2^T$, then there exists an orthogonal matrix $Q \in \mathbb{R}^{n \times n}$ with $Z_1 = Z_2 Q$ (see, e.g., [1]).

In the 2×2 case, the set of the orthogonal matrices is the union of all rotations and reflections in $\mathbb{R}^2$, which are expressed as

$$Q^1(\theta) = \begin{bmatrix} \sin\theta & -\cos\theta \\ \cos\theta & \sin\theta \end{bmatrix} \quad \text{and} \quad Q^{-1}(\theta) = \begin{bmatrix} \sin\theta & \cos\theta \\ \cos\theta & -\sin\theta \end{bmatrix}, \tag{11}$$

respectively, as θ varies in $]0,2\pi]$. Since $C = C^{1/2}(C^{1/2})^T = C^{1/2}C^{1/2}$ is a symmetric factorization of C, then all factorizations of C are given by

$$Z^{(\iota)}(\theta) = C^{1/2}Q^{(\iota)}(\theta) = \begin{bmatrix} \rho_{11} & \rho_{12} \\ \rho_{21} & \rho_{22} \end{bmatrix} Q^{(\iota)}(\theta) = \begin{bmatrix} z_{11}^{(\iota)}(\theta) & z_{12}^{(\iota)}(\theta) \\ z_{21}^{(\iota)}(\theta) & z_{22}^{(\iota)}(\theta) \end{bmatrix}, \tag{12}$$

where $\theta \in]0,2\pi]$ and $\iota \in \{-1,1\}$. In particular, we get

$$z_{11}^{(1)}(\theta) = z_{11}^{(-1)}(\theta), \quad z_{12}^{(1)}(\theta) = -z_{12}^{(-1)}(\theta), \quad z_{21}^{(1)}(\theta) = z_{21}^{(-1)}(\theta), \quad z_{22}^{(1)}(\theta) = -z_{22}^{(-1)}(\theta). \tag{13}$$

We assume that

$$C = x^T\, x = A\, s^T\, s\, A^T = A\, \widetilde{P}\, A^T, \tag{14}$$

where $\widetilde{P}$ is a symmetric and positive-definite estimate of the source derivative overlapping matrix P. In $\widetilde{P}$ we put

$$\widetilde{p}_{12} = \widetilde{p}_{21} = 0. \tag{15}$$

Observe that we do not assign a value to $\widetilde{p}_{11}$ and $\widetilde{p}_{22}$, as they will be determined later by imposing that the estimated mixture matrix is one row-sum. Let

$$\widetilde{P} = YY^T \tag{16}$$

be a symmetric factorization, where Y is a nonsingular matrix that satisfies

$$y_{11}\, y_{21} + y_{12}\, y_{22} = 0, \tag{17}$$

thanks to (15). From (14) and (16) we get

$$C \;=\; AYY^TA^T = AY(AY)^T,$$

that is, AY is a factorization of C. For every given choice of $\theta \in]0,2\pi]$ and $\iota \in \{-1,1\}$, we define an estimate $\widetilde{A}^{(\iota)}(\theta)$ of the mixture matrix A as a matrix such that $\widetilde{A}^{(\iota)}(\theta) = Z^{(\iota)}(\theta)Y^{-1}$, where $Z^{(\iota)}(\theta)$ is as in (12). We have

$$\begin{aligned} a_{11}^{(\iota)}(\theta) &= \frac{z_{11}^{(\iota)}(\theta)y_{22} - z_{12}^{(\iota)}(\theta)y_{21}}{y_{11}\,y_{22} - y_{21}\,y_{12}}, \qquad a_{12}^{(\iota)}(\theta) = \frac{z_{12}^{(\iota)}(\theta)y_{11} - z_{11}^{(\iota)}(\theta)y_{12}}{y_{11}\,y_{22} - y_{21}\,y_{12}}, \\ a_{21}^{(\iota)}(\theta) &= \frac{z_{21}^{(\iota)}(\theta)y_{22} - z_{22}^{(\iota)}(\theta)y_{21}}{y_{11}\,y_{22} - y_{21}\,y_{12}}, \qquad a_{22}^{(\iota)}(\theta) = \frac{z_{22}^{(\iota)}(\theta)y_{11} - z_{21}^{(\iota)}(\theta)y_{12}}{y_{11}\,y_{22} - y_{21}\,y_{12}}, \end{aligned} \tag{18}$$

and by imposing that $\widetilde{A}^{(\iota)}(\theta)$ satisfies the one row-sum condition in (3), we get

$$\begin{aligned} z_{11}^{(\iota)}(\theta)y_{22} - z_{12}^{(\iota)}(\theta)y_{21} + z_{12}^{(\iota)}(\theta)y_{11} - z_{11}^{(\iota)}(\theta)y_{12} &= y_{11}\,y_{22} - y_{21}\,y_{12}, \\ z_{21}^{(\iota)}(\theta)y_{22} - z_{22}^{(\iota)}(\theta)y_{21} + z_{22}^{(\iota)}(\theta)y_{11} - z_{21}^{(\iota)}(\theta)y_{12} &= y_{11}\,y_{22} - y_{21}\,y_{12}. \end{aligned} \tag{19}$$

Thus, the matrix Y fulfils the conditions in equations (17) and (19). The nonlinear system given by the equations (17) and (19) admits infinitely many solutions. For the sake of convenience, we choose the solution

$$\begin{aligned} y_{11} &= \frac{\det C}{(z_{22}^{(\iota)}(\theta) - z_{12}^{(\iota)}(\theta)) \det Z^{(\iota)}(\theta)}, & y_{12} &= 0, \\ y_{21} &= 0, & y_{22} &= \frac{\det Z^{(\iota)}(\theta)}{z_{11}^{(\iota)}(\theta) - z_{21}^{(\iota)}(\theta)}. \end{aligned} \tag{20}$$

This choice has several consequences. First, from (13) and (18) we obtain that $\widetilde{A}^{(1)}(\theta) = \widetilde{A}^{(-1)}(\theta)$ for all $\theta \in]0, 2\pi]$. Moreover, from equations (11) and (12) we get that $Z(\theta) = -Z(\theta + \pi)$, for $\theta \in]0, \pi]$, and hence from (18) and (20) we deduce that

$$\widetilde{A}(\theta) = \widetilde{A}(\theta + \pi), \tag{21}$$

for each $\theta \in]0, \pi]$.

So, in the following we consider only the case $\iota = 1$, we put $\widetilde{A}(\theta) = \widetilde{A}^{(1)}(\theta)$ and $Z(\theta) = Z^{(1)}(\theta)$ for each $\theta \in]0, \pi]$, and in general we consider only the values of θ belonging to $]0, \pi]$.

Recall that Y must be non-singular, since Y realizes a symmetric factorization of the non-singular matrix P.

Moreover, the equations in (20) are well defined if $z_{11}(\theta) \neq z_{21}(\theta)$ and $z_{12}(\theta) \neq z_{22}(\theta)$. In [1] we prove that $z_{11}(\theta) = z_{21}(\theta)$ or $z_{12}(\theta) = z_{22}(\theta)$ when θ assumes the values $\varphi + t\frac{\pi}{2}$, with $t \in \mathbb{Z}$ and

$$\varphi = \begin{cases} \arctan\left(\dfrac{\rho_{22} - \rho_{12}}{\rho_{11} - \rho_{21}}\right), & \text{if } \rho_{11} \neq \rho_{21}, \\ \dfrac{\pi}{2}, & \text{if } \rho_{11} = \rho_{21}, \end{cases} \tag{22}$$

where $\rho_{i,j}$, $i, j = 1, 2$, are the entries of the matrix $C^{1/2}$.

For any $\theta \in]\varphi, \varphi + \frac{\pi}{2}[\cup]\varphi + \frac{\pi}{2}, \varphi + \pi[$, we get that an estimate of the ideal sources s is given by

$$\widetilde{s}(\theta)^T = \begin{bmatrix} \widetilde{s}_r(\theta) & \widetilde{s}_v(\theta) \end{bmatrix}^T = \widetilde{A}^{-1}(\theta) x^T, \tag{23}$$

which, together with the fact that $\widetilde{A}^{-1}(\theta) = \widetilde{A}^1(\theta) = Z^{(1)}(\theta) Y^{-1}$ and (19), yields

$$\begin{aligned} \widetilde{s}_r(\theta) &= -\frac{z_{22}(\theta)}{z_{12}(\theta) - z_{22}(\theta)} x_r + \frac{z_{12}(\theta)}{z_{12}(\theta) - z_{22}(\theta)} x_v; \\ \widetilde{s}_v(\theta) &= -\frac{z_{21}(\theta)}{z_{11}(\theta) - z_{21}(\theta)} x_r + \frac{z_{11}(\theta)}{z_{11}(\theta) - z_{21}(\theta)} x_v. \end{aligned} \tag{24}$$

As we supposed that the derivatives of our estimated sources take values between 0 and $2m$, where m is the maximum value of the observed image, we take the orthogonal projection of the estimate $s_\iota(\theta)$ on the space $[0,2m]^{nm\times 2}$ with respect to the Frobenius norm. Namely, we apply to the estimate of the sources the function that maps a vector $s \in \mathbb{R}^{nm}$ to the nm-dimensional vector $\tau(s)$, whose elements are given by

$$(\tau(s))_i = \begin{cases} 0, & \text{if } s_i \leq 0, \\ s_i, & \text{if } 0 < s_i \leq 2m, \\ 2m, & \text{if } s_i > 2m, \end{cases} \qquad i = 1, \dots, nm. \tag{25}$$

By this transformation, the projections of the estimated source derivative images $\tau(\widetilde{s}_{r,\iota}(\theta))$ and $\tau(\widetilde{s}_{v,\iota}(\theta))$ turn to be nonnegative (see also [3, 5, 7, 14]). From now on, we consider the projections above as the new estimates of the derivatives of the sources. Thus, among the possible values of θ in $]\varphi, \varphi + \frac{\pi}{2}[\cup]\varphi + \frac{\pi}{2}, \varphi + \pi[$, we find a value $\widetilde{\theta}$ that minimizes the *objective function*

$$g(\theta, C) = \tau(\widetilde{s}_r(\theta))^T \cdot \tau(\widetilde{s}_v(\theta)). \tag{26}$$

Observe that from (21) and (23) it follows that the function g is periodic in the variable θ with period π. The function g is minimized by means of the algorithm given in [2].

The steps of the algorithm described in this section are illustrated as follows.

function ZEODS($\widehat{x}$)
determine the maximum value m of $\widehat{x}$;
$x = D\widehat{x}$;
$C = x^T x$;
$\widetilde{\theta} = argmin($**function** $g(\cdot, C))$;
$Z(\widetilde{\theta}) = C^{1/2} Q_1(\widetilde{\theta})$;
compute $\widetilde{s}_r(\widetilde{\theta})$ and $\widetilde{s}_v(\widetilde{\theta})$ as in (24);
return $D^{-1}\tau(\widetilde{s}(\widetilde{\theta}))$

The function $g(\cdot, \cdot)$ is computed as follows:

function $g(\theta, C)$
$Z(\theta) = C^{1/2} Q^1(\theta)$;
compute $\widetilde{s}_r(\theta)$ and $\widetilde{s}_v(\theta)$ as in (24);
return $(\tau(\widetilde{s}_r(\theta)))^T \cdot \tau(\widetilde{s}_v(\theta))$

We refer to this method as the *Zero Edge Overlapping in Document Separation* (ZEODS) algorithm, which is a parameter-free technique, and thus unsupervised.

4 Experimental results

We have used ideal images, from which the observed documents have been synthetically constructed from suitable mixture matrices. The ideal images used for the tests are represented in Figures 1 and 2.

(1.1) original recto

(1.2) original verso

(1.3) original recto

(1.4) original verso

(1.5) original recto

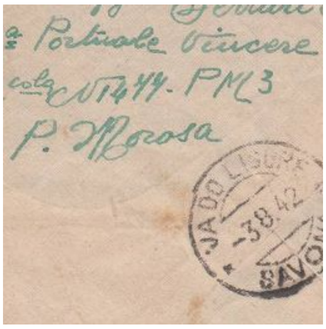

(1.6) original verso

Figure 1: Ideal images

In our tests, we have used both symmetric and asymmetric mixture matrices. In the following subsections, the obtained results are explained and compared with other techniques both computationally and from the graphical point of view. We examined RGB color images. The channels R, G and B was treated separately.

(2.1) original recto

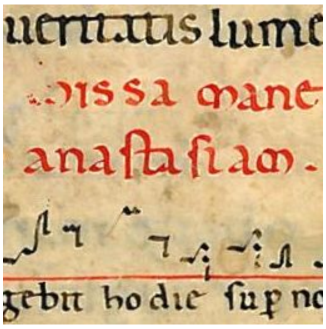

(2.2) original verso

(2.3) original recto

(2.4) original verso

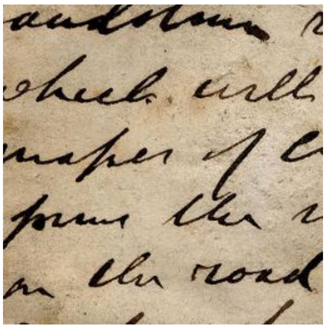

(2.5) original recto

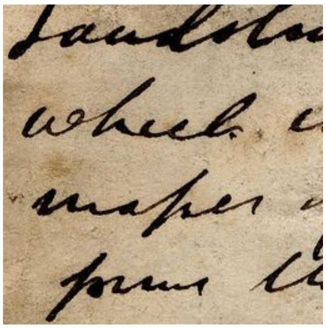

(2.6) original verso

Figure 2: Ideal images

4.1 Case 1: First symmetric matrix

The first case we investigate is a symmetric mixture matrix. For each channel R, G and B, the related matrices are

$$A_R = \begin{pmatrix} 0.6 & 0.4 \\ 0.4 & 0.6 \end{pmatrix}, \; A_G = \begin{pmatrix} 0.6 & 0.4 \\ 0.4 & 0.6 \end{pmatrix}, \; A_B = \begin{pmatrix} 0.6 & 0.4 \\ 0.4 & 0.6 \end{pmatrix}. \tag{27}$$

Now we see the behavior of the presented algorithms. We consider the ideal images in Figure 3, and using the above indicated mixture matrices, we synthetically obtain the degraded images in Figure 4.

(3.1) original recto

(3.2) original verso

Figure 3: Ideal images

(4.1) degraded recto

(4.2) degraded verso

Figure 4: Degraded images

By applying the algorithms we get, as estimates, the results in Figures 5-10.

In Table 1 we present the mean square errors with respect to the original documents obtained by means of the aforementioned algorithms for estimating the recto and the verso of Figure 3. Now we consider the following ideal images in Figure 11. Using the above indicated mixture matrices, we synthetically obtain the degraded images in Figure 12.

(5.1) recto estimated by ZEODS

(5.2) verso estimated by ZEODS

Figure 5: Estimates by ZEODS

(6.1) recto estimated by MATODS

(6.2) verso estimated by MATODS

Figure 6: Estimates by MATODS

(7.1) recto estimated by FastIca

(7.2) verso estimated by FastIca

Figure 7: Estimates by FastIca

(8.1) recto estimated by Symmetric Whitening

(8.2) verso estimated by Symmetric Whitening

Figure 8: Estimates by Symmetric Whitening

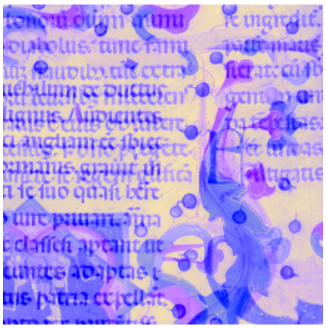

(9.1) recto estimated by Whitening

(9.2) verso estimated by Whitening

Figure 9: Estimates by Whitening

(10.1) recto estimated by PCA

(10.2) verso estimated by PCA

Figure 10: Estimates by PCA

Used Technique	MSE Recto	MSE Verso	MSE of A
ZEODS	5.0766	0.6228	$1.020 \cdot 10^{-4}$
MATODS	12.5173	49.0506	0.0011
FASTICA	58.2382	212.8663	0.0546
Symmetric Whitening	428.0422	373.6753	0.00183
Whitening	$7.7086 \cdot 10^{3}$	$6.2362 \cdot 10^{3}$	0.3561
PCA	$1.4943 \cdot 10^{4}$	$5.2861 \cdot 10^{3}$	0.3770

Table 1: Errors of the algorithms by using the mixture matrix in (27).

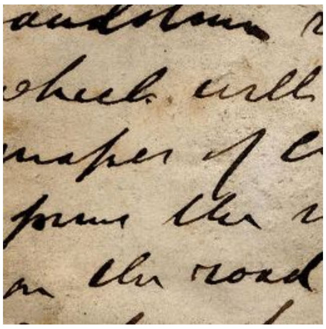

(11.1) original recto

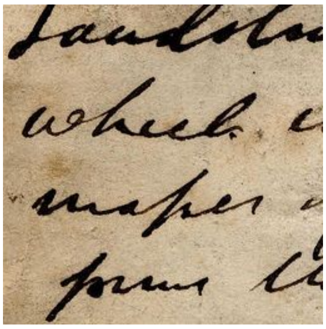

(11.2) original verso

Figure 11: Ideal images

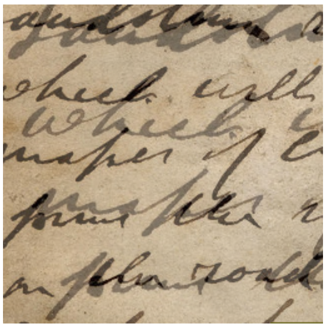

(12.1) degraded recto

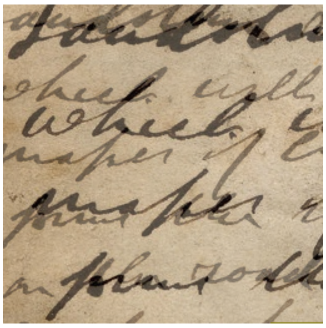

(12.2) degraded verso

Figure 12: Degraded images

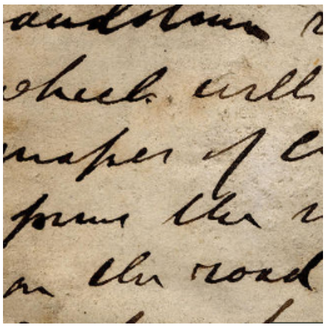

(13.1) recto estimated by ZEODS

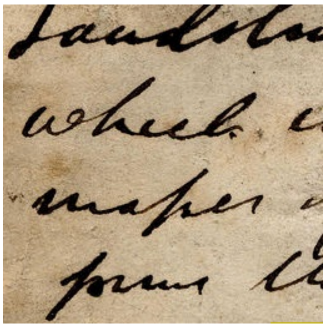

(13.2) verso estimated by ZEODS

Figure 13: Estimates by ZEODS

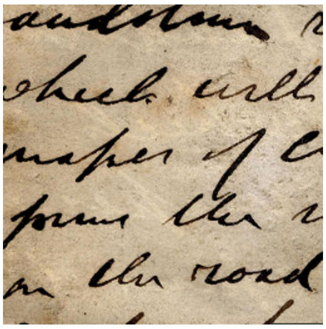

(14.1) recto estimated by MATODS

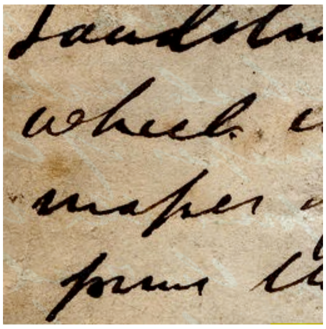

(14.2) verso estimated by MATODS

Figure 14: Estimates by MATODS

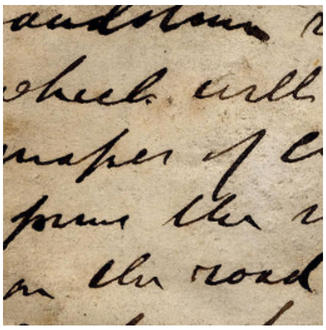

(15.1) recto estimated by FastIca

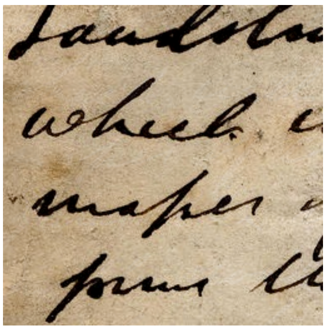

(15.2) verso estimated by FastIca

Figure 15: Estimates by FastIca

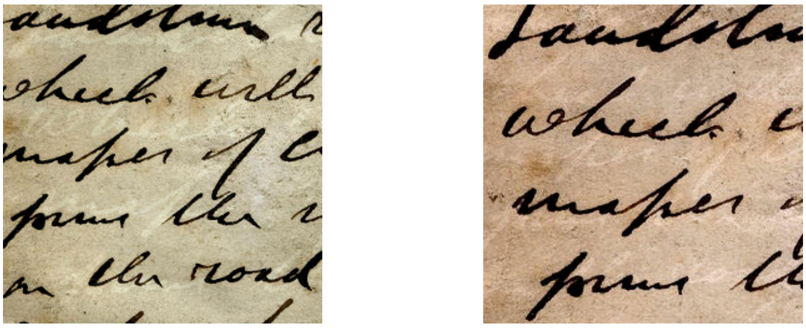

(16.1) recto estimated by Symmetric Whitening

(16.2) verso estimated by Symmetric Whitening

Figure 16: Estimates by Symmetric Whitening

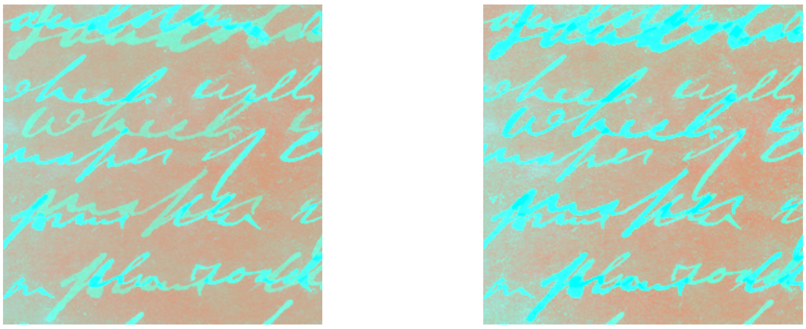

(17.1) recto estimated by Whitening

(17.2) verso estimated by Whitening

Figure 17: Estimates by Whitening

(18.1) recto estimated by PCA

(18.2) verso estimated by PCA

Figure 18: Estimates by PCA

By applying the algorithms we obtain, as estimates, the results in Figures 13-18.

In Table 2 we give the mean square errors with respect to the original documents obtained by means of the above algorithms for the estimates of the recto and the verso of Figure 11.

Used Technique	MSE Recto	MSE Verso	MSE of A
ZEODS	1.7592	0.4784	$5.4688 \cdot 10^{-5}$
MATODS	25.6900	52.0605	$1.2550 \cdot 10^{-4}$
FASTICA	3.3840	3.4516	0.0095
Symmetric Whitening	74.7709	80.8914	0.0110
Whitening	$8.4391 \cdot 10^3$	$5.98950 \cdot 10^3$	0.4561
PCA	$1.4068 \cdot 10^4$	$3.9386 \cdot 10^3$	0.4225

Table 2: Errors of the algorithms by using the mixture matrix in (27).

We consider the ideal images in Figure 19.

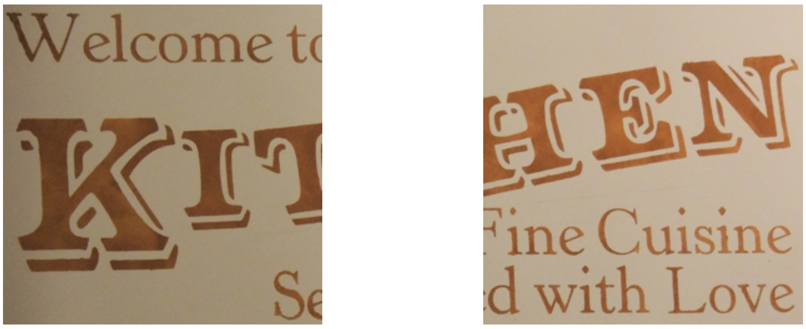

(19.1) original recto

(19.2) original verso

Figure 19: Ideal images

Using the above indicated mixture matrices, we synthetically obtain the degraded images in Figure 20.

By applying the algorithms we obtain, as estimates, the results in Figures 21-26.

In Table 3 we present the mean square errors with respect to the original documents obtained by means of the above algorithms for the estimate of the recto and the verso of Figure 19. We consider the ideal images in Figure 27.

Using the above indicated mixture matrices, we synthetically obtain the degraded images in Figure 28.

By applying the algorithms we obtain, as estimates, the results in Figures 29-34.

In Table 4 we indicate the mean square errors with respect to the original documents obtained by means of the above algorithms for the estimate of the recto and the verso of

(20.1) degraded recto

(20.2) degraded verso

Figure 20: Degraded images

(21.1) recto estimated by ZEODS

(21.2) verso estimated by ZEODS

Figure 21: Estimates by ZEODS

(22.1) recto estimated by MATODS

(22.2) verso estimated by MATODS

Figure 22: Estimates by MATODS

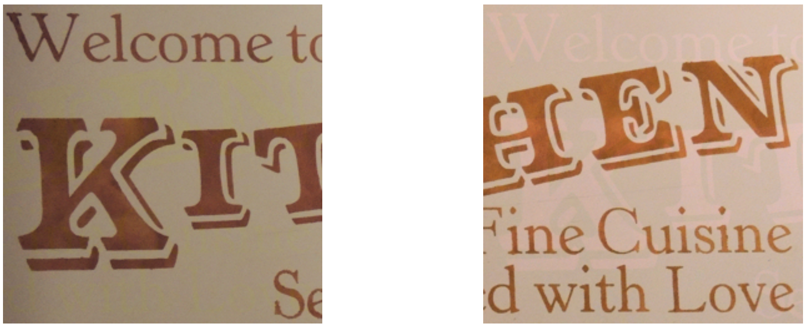

(23.1) recto estimated by FastIca

(23.2) verso estimated by FastIca

Figure 23: Estimates by FastIca

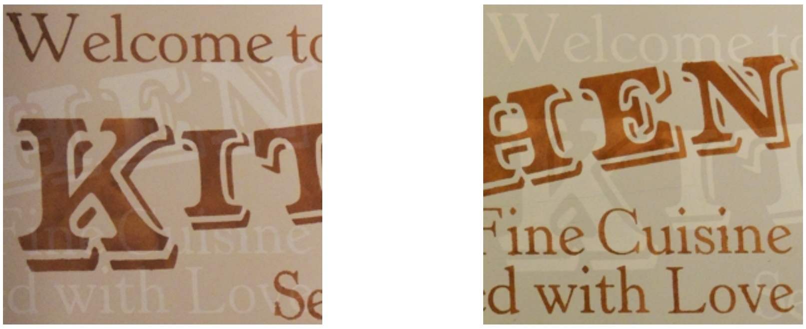

(24.1) recto estimated by Symmetric Whitening

(24.2) verso estimated by Symmetric Whitening

Figure 24: Estimates by Symmetric Whitening

(25.1) recto estimated by Whitening

(25.2) verso estimated by Whitening

Figure 25: Estimates by Whitening

(26.1) recto estimated by PCA

(26.2) verso estimated by PCA

Figure 26: Estimates by PCA

Used Technique	MSE Recto	MSE Verso	MSE of A
ZEODS	0.8752	0.6474	$4.4766 \cdot 10^{-5}$
MATODS	172.146	180.0660	$2.8565 \cdot 10^{-4}$
FASTICA	12.1634	43.6463	0.0395
Symmetric Whitening	261.5776	259.4301	0.00168
Whitening	$3.5723 \cdot 10^{3}$	$1.5907 \cdot 10^{3}$	0.4596
PCA	$5.9609 \cdot 10^{3}$	$1.4281 \cdot 10^{3}$	0.4242

Table 3: Errors of the algorithms by using the mixture matrix in (27).

(27.1) original recto

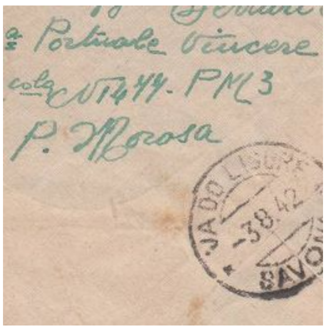

(27.2) original verso

Figure 27: Ideal images

(28.1) degraded recto

(28.2) degraded verso

Figure 28: Degraded images

(29.1) recto estimated by ZEODS

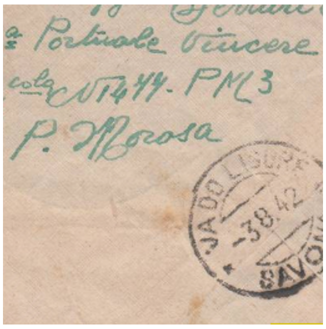

(29.2) verso estimated by ZEODS

Figure 29: Estimates by ZEODS

(30.1) recto estimated by MATODS

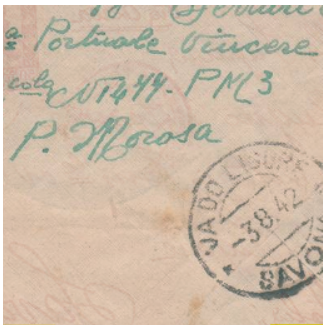

(30.2) verso estimated by MATODS

Figure 30: Estimates by MATODS

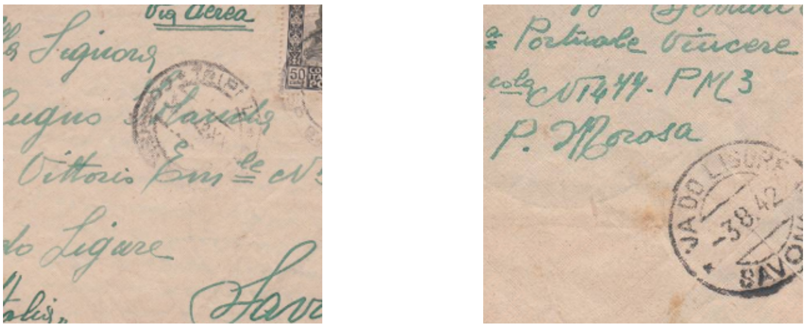

(31.1) recto estimated by FastIca

(31.2) verso estimated by FastIca

Figure 31: Estimates by FastIca

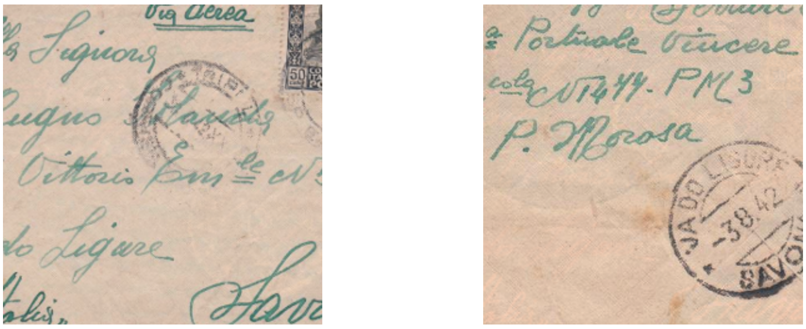

(32.1) recto estimated by Symmetric Whitening

(32.2) verso estimated by Symmetric Whitening

Figure 32: Estimates by Symmetric Whitening

(33.1) recto estimated by Whitening

(33.2) verso estimated by Whitening

Figure 33: Estimates by Whitening

(34.1) recto estimated by PCA

(34.2) verso estimated by PCA

Figure 34: Estimates by PCA

Figure 27.

Used Technique	MSE Recto	MSE Verso	MSE of A
ZEODS	0.7829	0.5673	$1.095 \cdot 10^{-4}$
MATODS	0.9015	10.3131	0.0014
FASTICA	1.0849	0.6707	0.0136
Symmetric Whitening	8.5123	12.2799	0.0085
Whitening	$1.9433 \cdot 10^3$	$1.2006 \cdot 10^3$	0.4548
PCA	$2.9914 \cdot 10^3$	$716.5649 \cdot 10^3$	0.4234

Table 4: Errors of the algorithms by using the mixture matrix in (27).

We consider the ideal images in Figure 35.

Using the above indicated mixture matrices, we synthetically obtain the degraded images in Figure 36.

By applying the algorithms we obtain, as estimates, the results in Figures 37-42.

In Table 5 we present the mean square errors with respect to the original documents obtained by means of the above algorithms for the estimate of the recto and the verso of Figure 35.

As we can observe from the results of the previous subsection, the proposed and implemented ZEODS method obtains better results than algorithms FastIca, PCA, Whitening and Symmetric Whitening. However the MATODS algorithm obtains results close to those of the ZEODS algorithm only in the image in Figure 27. To see this, we compare the execution time of the two algorithms in the image in Figure 27. The results are presented in Table 14.

To see a further demonstration of what we said before, we now make a further test on another image, obtaining similar results by means of both algorithms obtaining similar results

(35.1) original recto

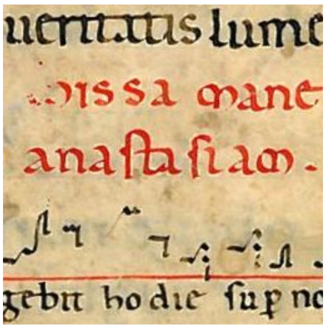

(35.2) original verso

Figure 35: Ideal images

(36.1) degraded recto

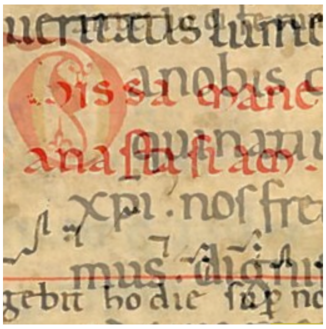

(36.2) degraded verso

Figure 36: Degraded images

(37.1) recto estimated by ZEODS

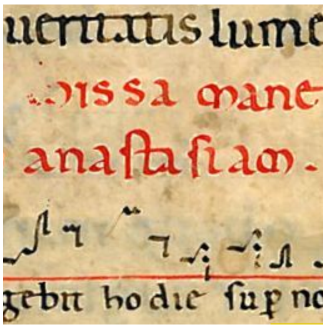

(37.2) verso estimated by ZEODS

Figure 37: Estimates by ZEODS

(38.1) recto estimated by MATODS

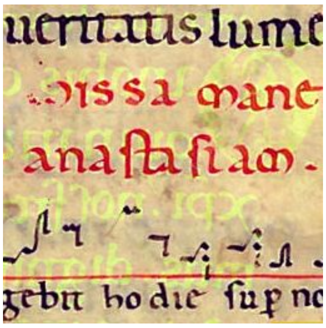

(38.2) verso estimated by MATODS

Figure 38: Estimates by MATODS

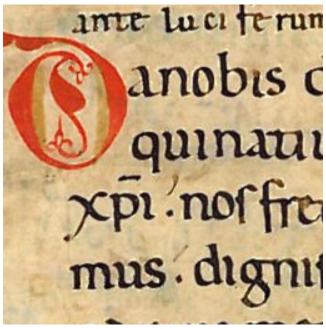

(39.1) recto estimated by FastIca

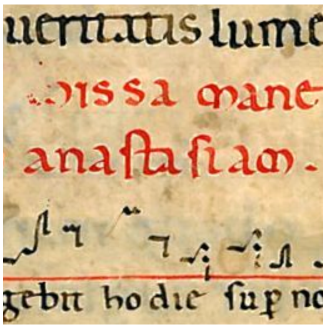

(39.2) verso estimated by FastIca

Figure 39: Estimates by FastIca

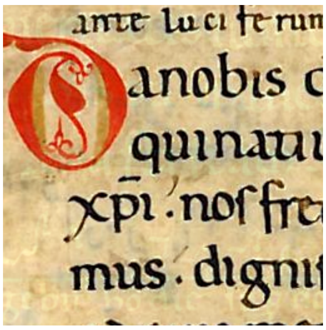

(40.1) recto estimated by Symmetric Whitening

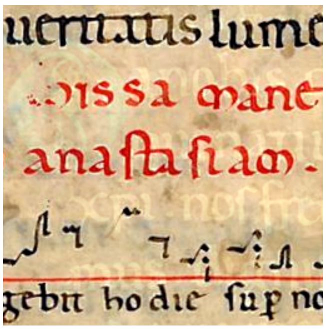

(40.2) verso estimated by Symmetric Whitening

Figure 40: Estimates by Symmetric Whitening

(41.1) recto estimated by Whitening

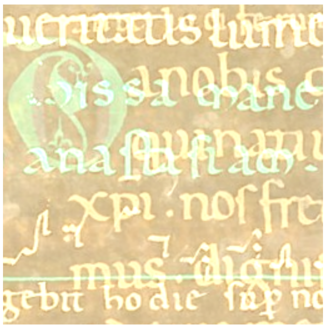

(41.2) verso estimated by Whitening

Figure 41: Estimates by Whitening

(42.1) recto estimated by PCA

(42.2) verso estimated by PCA

Figure 42: Estimates by PCA

Used Technique	MSE Recto	MSE Verso	MSE of A
ZEODS	4.7486	1.6165	$1.4055 \cdot 10^{-4}$
MATODS	136.7090	120.7570	0.0015
FASTICA	58.2382	212.8663	0.0546
Symmetric Whitening	428.0422	373.6753	0.0183
Whitening	$7.7086 \cdot 10^3$	$6.2362 \cdot 10^3$	0.3561
PCA	$1.4943 \cdot 10^4$	$5.2861 \cdot 10^3$	0.3770

Table 5: Errors of the algorithms by using the mixture matrix in (27).

Used Technique	Time
ZEODS	$0.3320s$
MATODS	$754.1420s$

Table 6: Execution time of the algorithms MATODS and ZEODS by using the mixture matrix in (27) on the image in Figure 27

by means of both algorithms ZEODS and MATODS.

We consider the ideal images in Figure 43.

(43.1) original recto

(43.2) original verso

Figure 43: Ideal images

Using the above indicated mixture matrices, we synthetically obtain the degraded images in Figure 44.

(44.1) degraded recto

(44.2) degraded verso

Figure 44: Degraded images

In Table 7 we present the mean square errors with respect to the original documents obtained by means of the above algorithms for the estimate of the recto and the verso of Figure 43.

The algorithms MATODS and ZEODS obtain very similar results. By applying the algorithms we obtain, as estimates, the results in Figures 45-46. Now we analyze the execution time of the algorithms. As in the previous case, we see that the ZEODS method gives results in a much shorter time than the MATODS method, as shown in Table 14.

These results given in terms of time are consistent with the previously obtained results.

Used Technique	MSE Recto	MSE Verso	MSE of A
ZEODS	0.0008	0.4494	$1.6842 \cdot 10^{-6}$
MATODS	0.0081	0.0019	$1.29 \cdot 10^{-4}$
FASTICA	42.7700	70.7900	0.0066
Symmetric Whitening	341.69	342.1863	0.0048
Whitening	245.8900	262.93	0.0086
PCA	$9249 \cdot 10^4$	$10330 \cdot 10^3$	0.038

Table 7: Errors of the algorithms by using the mixture matrix in (27).

(45.1) recto estimated by ZEODS

(45.2) verso estimated by ZEODS

Figure 45: Estimates by ZEODS

(46.1) recto estimated by MATODS

(46.2) verso estimated by MATODS

Figure 46: Estimates by MATODS

Used Technique	Time
ZEODS	$0.3410s$
MATODS	$750.6980s$

Table 8: Execution time of the algorithms MATODS and ZEODS by using the mixture matrix in (27) on the image in Figure 43

4.2 Case 2: Second symmetric matrix

The second case we investigate is another symmetric mixture matrix. For every channel R, G and B, the corresponding matrices are

$$A_R = \begin{pmatrix} 0.7 & 0.3 \\ 0.3 & 0.7 \end{pmatrix}, \; A_G = \begin{pmatrix} 0.7 & 0.3 \\ 0.3 & 0.7 \end{pmatrix}, \; A_B = \begin{pmatrix} 0.7 & 0.3 \\ 0.3 & 0.7 \end{pmatrix}. \tag{28}$$

Now we see the behavior of the presented algorithms, in connection both with errors and with the graphical point of view.

We consider the ideal images in Figure 47.

(47.1) original recto

(47.2) original verso

Figure 47: Ideal images

Using the above indicated mixture matrices, we synthetically obtain the degraded images in Figure 48.

(48.1) degraded recto

(48.2) degraded verso

Figure 48: Degraded images

By applying the algorithms we obtain, as estimates, the results in Figures 49-54. In Table 9 we present the mean square errors with respect to the original documents obtained by means of the above algorithms for the estimate of the recto and the verso of Figure 47.

(49.1) recto estimated by ZEODS

(49.2) verso estimated by ZEODS

Figure 49: Estimates by ZEODS

(50.1) recto estimated by MATODS

(50.2) verso estimated by MATODS

Figure 50: Estimates by MATODS

(51.1) recto estimated by FastIca

(51.2) verso estimated by FastIca

Figure 51: Estimates by FastIca

(52.1) recto estimated by Symmetric Whitening

(52.2) verso estimated by Symmetric Whitening

Figure 52: Estimates by Symmetric Whitening

(53.1) recto estimated by Whitening

(53.2) verso estimated by Whitening

Figure 53: Estimates by Whitening

(54.1) recto estimated by PCA

(54.2) verso estimated by PCA

Figure 54: Estimates by PCA

Used Technique	MSE Recto	MSE Verso	MSE of A
ZEODS	0.8547	4.9596	$5.8836 \cdot 10^{-5}$
MATODS	17.6269	50.6982	0.0004
FASTICA	37.5413	86.2744	0.0783
Symmetric Whitening	519.4615	288.9082	0.0352
Whitening	$2.4090 \cdot 10^{3}$	400.2690	0.0352
PCA	$7.7310 \cdot 10^{3}$	$3.7087 \cdot 10^{3}$	0.3674

Table 9: Errors of the algorithms by using the mixture matrix in (28).

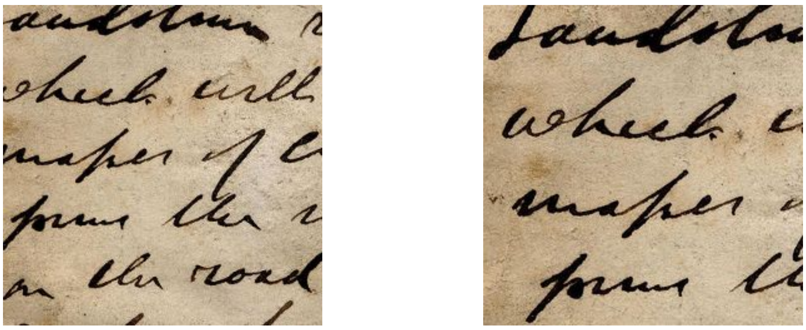

(55.1) original recto (55.2) original verso

Figure 55: Ideal images

We consider the ideal images in Figure 55. Using the above mixture matrices, we synthetically obtain the degraded images in Figure 56.

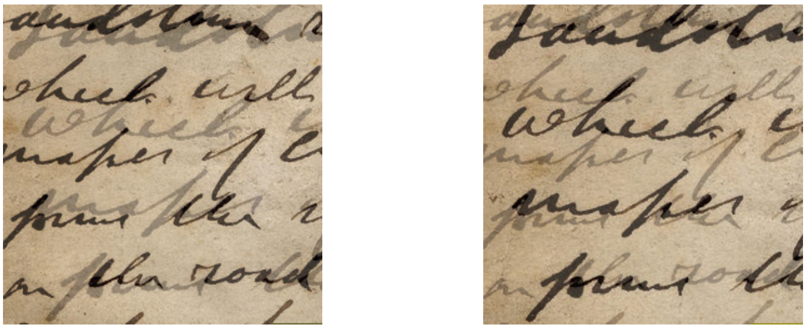

(56.1) degraded recto (56.2) degraded verso

Figure 56: Degraded images

By applying the algorithms we obtain, as estimates, the results in Figures 57-62.

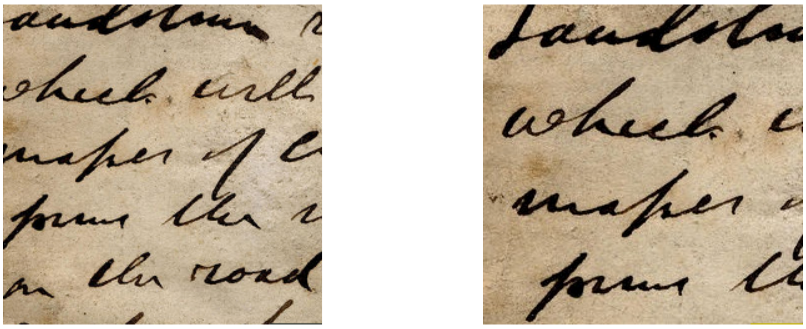

(57.1) recto estimated by ZEODS (57.2) verso estimated by ZEODS

Figure 57: Estimates by ZEODS

In Table 10 we present the mean square errors with respect to the original documents obtained by means of the above algorithms for the estimate of the recto and the verso of Figure 55.

We consider the ideal images in Figure 63.

Using the above indicated mixture matrices, we synthetically obtain the degraded images in Figure 64.

By applying the algorithms we obtain, as estimates, the results in Figures 65-70.

In Table 11 we present the mean square errors with respect to the original documents obtained by means of the above algorithms for the estimate of the recto and the verso of Figure 63. We consider the ideal images in Figure 71.

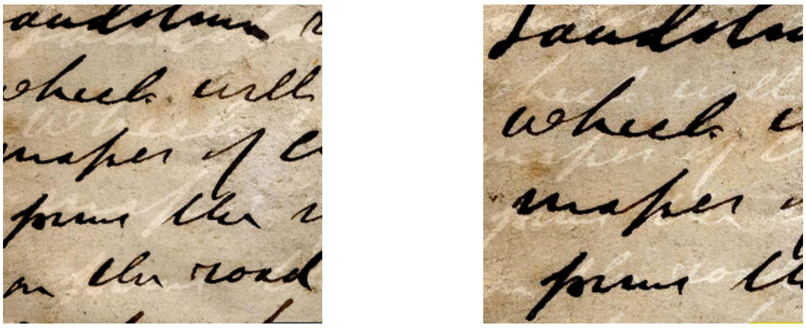

(58.1) recto estimated by MATODS

(58.2) verso estimated by MATODS

Figure 58: Estimates by MATODS

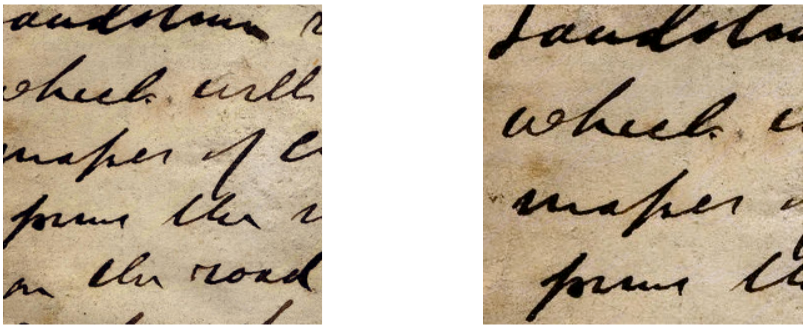

(59.1) recto estimated by FastIca

(59.2) verso estimated by FastIca

Figure 59: Estimates by FastIca

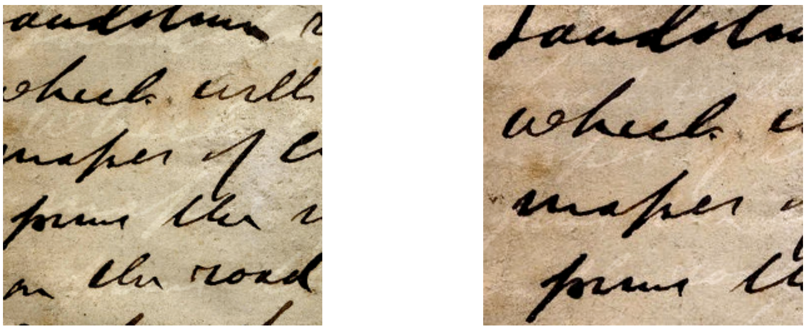

(60.1) recto estimated by Symmetric Whitening

(60.2) verso estimated by Symmetric Whitening

Figure 60: Estimates by Symmetric Whitening

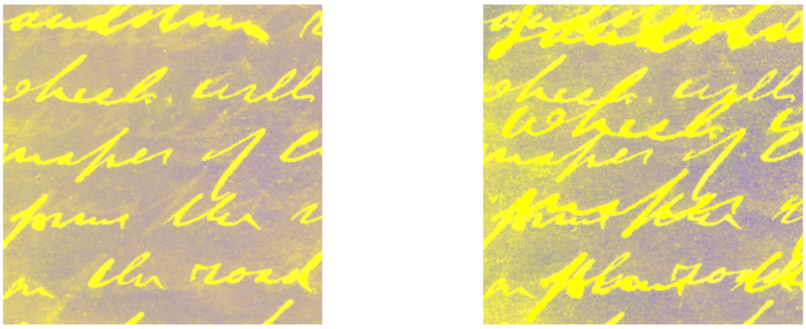

(61.1) recto estimated by Whitening

(61.2) verso estimated by Whitening

Figure 61: Estimates by Whitening

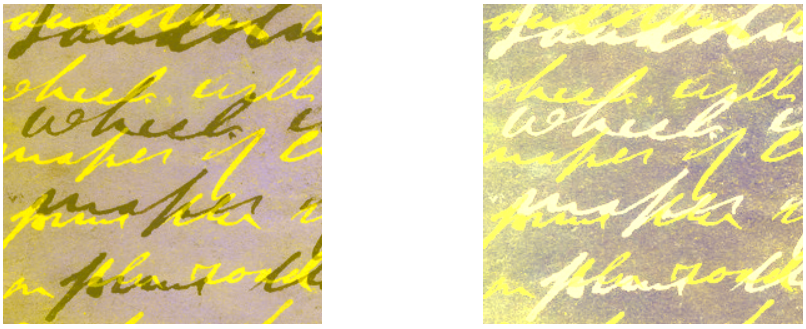

(62.1) recto estimated by PCA

(62.2) verso estimated by PCA

Figure 62: Estimates by PCA

Used Technique	MSE Recto	MSE Verso	MSE of A
ZEODS	0.0648	2.9075	$1.3883 \cdot 10^{-5}$
MATODS	125.8860	213.165	0.0035
FASTICA	14.2089	1.7185	0.0215
Symmetric Whitening	71.8710	75.6985	0.224
Whitening	$1.1589 \cdot 10^{4}$	$6.9410 \cdot 10^{3}$	0.4281
PCA	$1.5428 \cdot 10^{4}$	$5.3671 \cdot 10^{3}$	0.4305

Table 10: Errors of the algorithms by using the mixture matrix in (28).

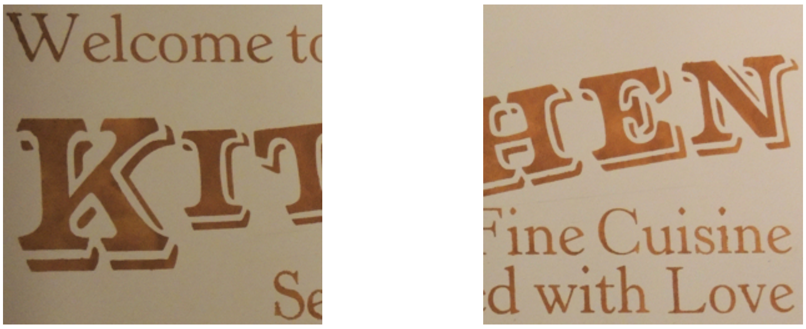

(63.1) original recto

(63.2) original verso

Figure 63: Ideal images

(64.1) degraded recto

(64.2) degraded verso

Figure 64: Degraded images

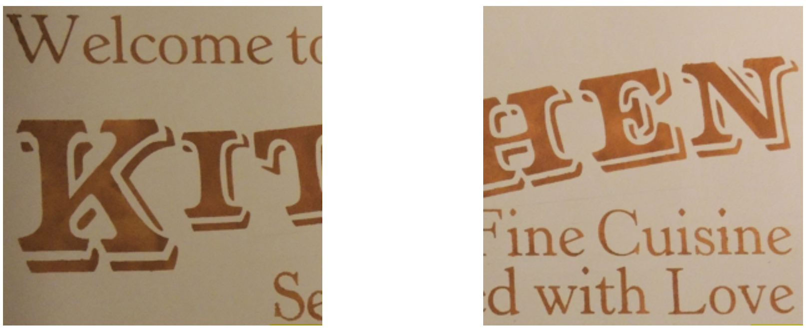

(65.1) recto estimated by ZEODS

(65.2) verso estimated by ZEODS

Figure 65: Estimates by ZEODS

(66.1) recto estimated by MATODS

(66.2) verso estimated by MATODS

Figure 66: Estimates by MATODS

(67.1) recto estimated by FastIca

(67.2) verso estimated by FastIca

Figure 67: Estimates by FastIca

(68.1) recto estimated by Symmetric Whitening

(68.2) verso estimated by Symmetric Whitening

Figure 68: Estimates by Symmetric Whitening

(69.1) recto estimated by Whitening

(69.2) verso estimated by Whitening

Figure 69: Estimates by Whitening

(70.1) recto estimated by PCA

(70.2) verso estimated by PCA

Figure 70: Estimates by PCA

Used Technique	MSE Recto	MSE Verso	MSE of A
ZEODS	0.7132	1.8467	$2.1718 \cdot 10^{-5}$
MATODS	12.4361	48.8206	0.021
FASTICA	12.2312	42.1443	0.0407
Symmetric Whitening	190.6356	174.7290	0.0326
Whitening	$3.9342 \cdot 10^{3}$	$1.5761 \cdot 10^{3}$	0.4392
PCA	$5.7594 \cdot 10^{3}$	$1.5845 \cdot 10^{3}$	0.4368

Table 11: Errors of the algorithms by using the mixture matrix in (28).

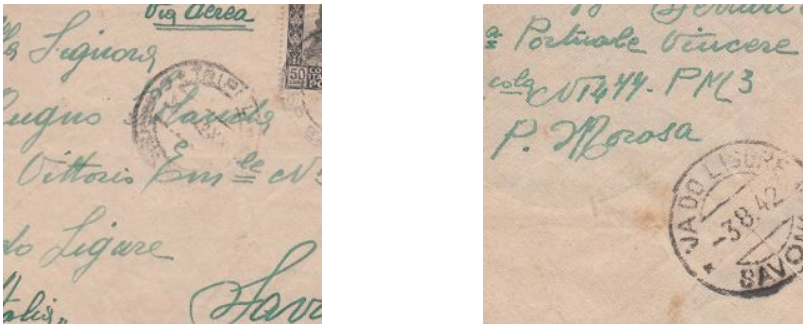

(71.1) original recto (71.2) original verso

Figure 71: Ideal images

Using the above indicated mixture matrices, we synthetically obtain the degraded images in Figure 72.

(72.1) degraded recto (72.2) degraded verso

Figure 72: Degraded images

By applying the algorithms we obtain, as estimates, the results in Figures 73-78.

In Table 12 we present the mean square errors with respect to the original documents obtained by means of the above algorithms for the estimate of the recto and the verso of Figure 71.

We consider the ideal images in Figure 79.

Using the above indicated mixture matrices, we synthetically obtain the degraded images in Figure 80.

By applying the algorithms we obtain, as estimates, the results in Figures 81-86.

In Table 13 we present the mean square errors with respect to the original documents obtained by means of the above algorithms for the estimate of the recto and the verso of Figure 79 and the corresponding distance between the ideal and the estimated sources.

As we can note in the results of the previous subsection, the ZEODS methods, in terms of errors, always obtains better results than the FastIca, PCA, Whitening and Symmetric

(73.1) recto estimated by ZEODS

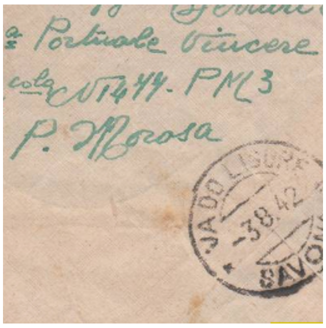

(73.2) verso estimated by ZEODS

Figure 73: Estimates by ZEODS

(74.1) recto estimated by MATODS

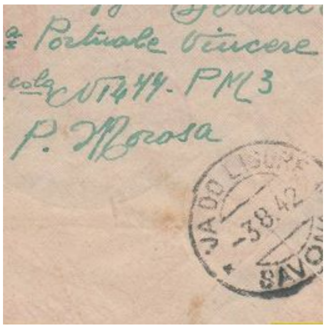

(74.2) verso estimated by MATODS

Figure 74: Estimates by MATODS

(75.1) recto estimated by FastIca

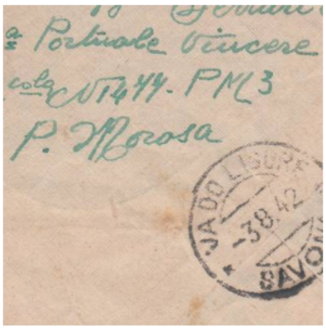

(75.2) verso estimated by FastIca

Figure 75: Estimates by FastIca

(76.1) recto estimated by Symmetric Whitening

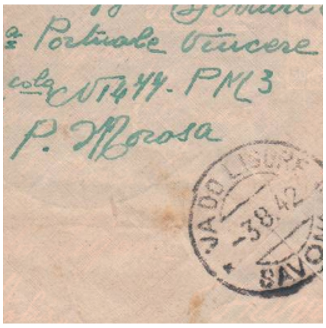

(76.2) verso estimated by Symmetric Whitening

Figure 76: Estimates by Symmetric Whitening

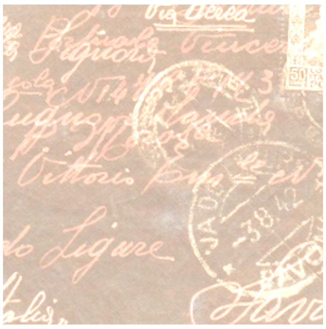

(77.1) recto estimated by Whitening

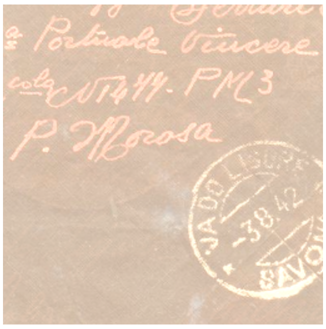

(77.2) verso estimated by Whitening

Figure 77: Estimates by Whitening

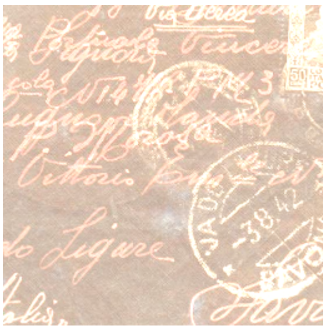

(78.1) recto estimated by PCA

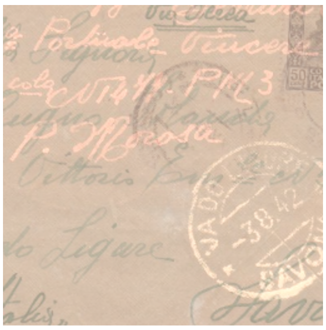

(78.2) verso estimated by PCA

Figure 78: Estimates by PCA

Used Technique	MSE Recto	MSE Verso	MSE of A
ZEODS	0.2304	1.9043	$5.5429 \cdot 10^{-5}$
MATODS	1.4521	3.5621	0.0010
FASTICA	0.8686	0.4879	0.0120
Symmetric Whitening	5.1557	10.1508	0.0159
Whitening	$2.8938 \cdot 10^{3}$	$1.5686 \cdot 10^{3}$	0.5148
PCA	$3.5387 \cdot 10^{3}$	$1.0885 \cdot 10^{3}$	0.4658

Table 12: Errors of the algorithms by using the mixture matrix in (28).

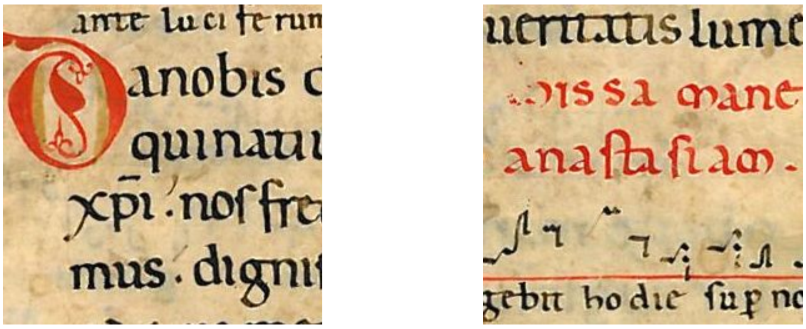

(79.1) original recto (79.2) original verso

Figure 79: Ideal images

(80.1) degraded recto (80.2) degraded verso

Figure 80: Degraded images

(81.1) recto estimated by ZEODS

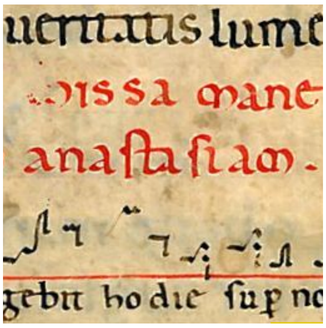

(81.2) verso estimated by ZEODS

Figure 81: Estimates by ZEODS

(82.1) recto estimated by MATODS

(82.2) verso estimated by MATODS

Figure 82: Estimates by MATODS

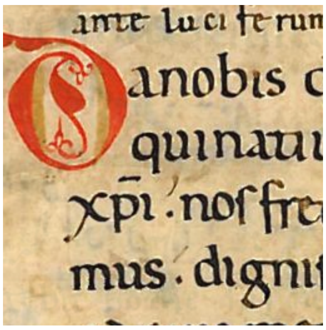

(83.1) recto estimated by FastIca

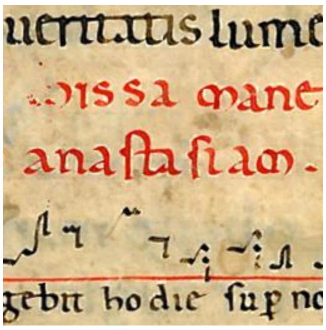

(83.2) verso estimated by FastIca

Figure 83: Estimates by FastIca

(84.1) recto estimated by Symmetric Whitening

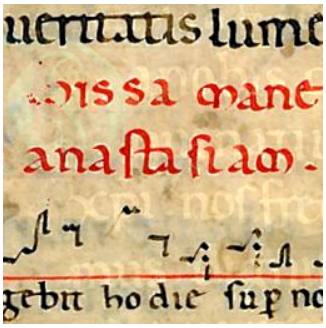

(84.2) verso estimated by Symmetric Whitening

Figure 84: Estimates by Symmetric Whitening

(85.1) recto estimated by Whitening

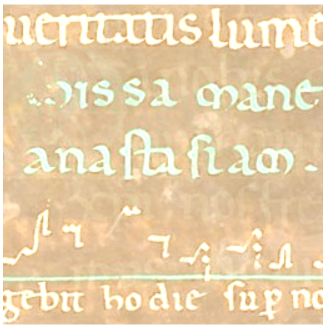

(85.2) verso estimated by Whitening

Figure 85: Estimates by Whitening

(86.1) recto estimated by PCA

(86.2) verso estimated by PCA

Figure 86: Estimates by PCA

Used Technique	MSE Recto	MSE Verso	MSE of A
ZEODS	1.6564	4.5617	$9.4655 \cdot 10^{-5}$
MATODS	110.2154	85.9412	0.0015
FASTICA	19.2557	7.4678	0.0266
Symmetric Whitening	31.9505	84.1863	0.0220
Whitening	$1.8337 \cdot 10^4$	$8.4063 \cdot 10^3$	0.5216
PCA	$2.2485 \cdot 10^4$	$5.9284 \cdot 10^3$	0.4693

Table 13: Errors of the algorithms by using the mixture matrix in (28).

Whitening algorithms. However the MATODS algorithm obtains results close to those of the proposed algorithm only in the image in Figure 71. But the execution time of the ZEODS algorithm is much shorter than those of the MATODS algorithm. To see this, we compare the execution time of the two algorithms in the image in Figure 71.

Used Technique	Time
ZEODS	$0.3150s$
MATODS	$687.3250s$

Table 14: Execution time of the algorithms MATODS and ZEODS by using the mixture matrix in (28) on the image in Figure 71

To see a further demonstration of what we said before, we now make a further test on another image, obtaining similar results by means of both algorithms ZEODS e MATODS.

We consider the ideal images in Figure 87.

(87.1) original recto

(87.2) original verso

Figure 87: Ideal images

Using the above indicated mixture matrices, we synthetically obtain the degraded images in Figure 88.

(88.1) degraded recto

(88.2) degraded verso

Figure 88: Degraded images

In Table 15 we present the mean square errors with respect to the original documents obtained by means of the above algorithms for the estimate of the recto and the verso of Figure 87. The algorithms MATODS and ZEODS obtain very similar results. We obtain,

Used Technique	MSE Recto	MSE Verso	MSE of A
ZEODS	5.2751	4.1563	$4.1236 \cdot 10^{-5}$
MATODS	0.1501	0.1910	$1.4301 \cdot 10^{-5}$
FASTICA	42.7700	70.7900	0.0066
Symmetric Whitening	341.69	342.1863	0.0048
Whitening	245.8900	262.93	0.0086
PCA	9249	10330	0.038

Table 15: Errors of the algorithms by using the mixture matrix in (28).

as estimates, the results in Figures 89-90. However, if we analyze the excution time of the algorithm, we see that the ZEODS method gives results in a much shorter time than the MATODS method, as shown in Table 16.

Used Technique	Time
ZEODS	$0.3330s$
MATODS	$489.0880s$

Table 16: Execution time of the algorithms MATODS and ZEODS by using the mixture matrix in (28).

(89.1) recto estimated by ZEODS

(89.2) verso estimated by ZEODS

Figure 89: Estimates by ZEODS

(90.1) recto estimated by MATODS

(90.2) verso estimated by MATODS

Figure 90: Estimates by MATODS

4.3 Case 3: First asymmetric matrix

The third case we deal with is an asymmetric mixture matrix. For every channel R, G and B, the related matrices are

$$A_R = \begin{pmatrix} 0.7 & 0.3 \\ 0.3 & 0.7 \end{pmatrix}, \; A_G = \begin{pmatrix} 0.7 & 0.3 \\ 0.2 & 0.8 \end{pmatrix}, \; A_B = \begin{pmatrix} 0.6 & 0.4 \\ 0.3 & 0.7 \end{pmatrix}. \tag{29}$$

Now we see the behavior of the presented algorithms, concerning both errors and the graphical point of view.

We consider the ideal images in Figure 91.

(91.1) original recto (91.2) original verso

Figure 91: Ideal images

Using the above indicated mixture matrices, we synthetically obtain the degraded images in Figure 92.

(92.1) degraded recto (92.2) degraded verso

Figure 92: Degraded images

By applying the algorithms we obtain, as estimates, the results in Figures 93-98.

In Table 17 we present the mean square errors with respect to the original documents obtained by means of the above algorithms for the estimate of the recto and the verso of

(93.1) recto estimated by ZEODS

(93.2) verso estimated by ZEODS

Figure 93: Estimates by ZEODS

(94.1) recto estimated by MATODS

(94.2) verso estimated by MATODS

Figure 94: Estimates by MATODS

(95.1) recto estimated by FastIca

(95.2) verso estimated by FastIca

Figure 95: Estimates by FastIca

(96.1) recto estimated by Symmetric Whitening

(96.2) verso estimated by Symmetric Whitening

Figure 96: Estimates by Symmetric Whitening

(97.1) recto estimated by Whitening

(97.2) verso estimated by Whitening

Figure 97: Estimates by Whitening

(98.1) recto estimated by PCA

(98.2) verso estimated by PCA

Figure 98: Estimates by PCA

Used Technique	MSE Recto	MSE Verso	MSE of A
ZEODS	0.9539	3.8356	$6.1210 \cdot 10^{-5}$
MATODS	45.2314	49.0506	0.0011
FASTICA	29.2027	148.9813	0.0701
Symmetric Whitening	451.6652	419.6792	0.0373
Whitening	$2.8741 \cdot 10^3$	352.5680	0.1792
PCA	$8.0327 \cdot 10^3$	$3.5478 \cdot 10^3$	0.3596

Table 17: Errors of the algorithms by using the mixture matrix in (29).

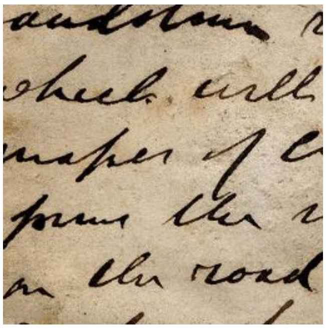

(99.1) original recto

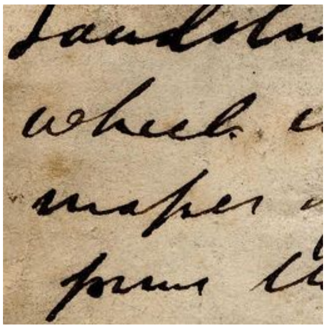

(99.2) original verso

Figure 99: Ideal images

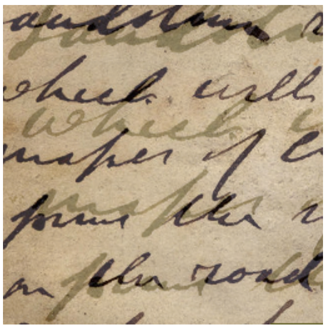

(100.1) degraded recto

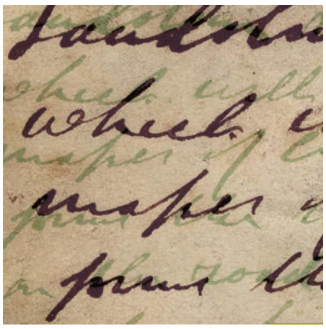

(100.2) degraded verso

Figure 100: Degraded images

Figure 91. We consider the ideal images in Figure 99. Using the above indicated mixture matrices, we synthetically obtain the degraded images in Figure 100.

By applying the algorithms we obtain, as estimates, the results in Figures 101-106.

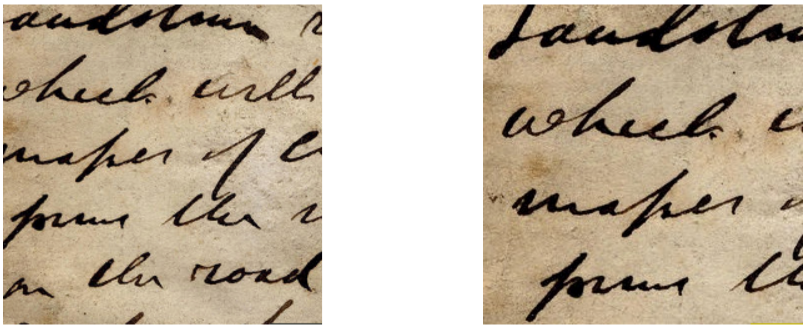

(101.1) recto estimated by ZEODS

(101.2) verso estimated by ZEODS

Figure 101: Estimates by ZEODS

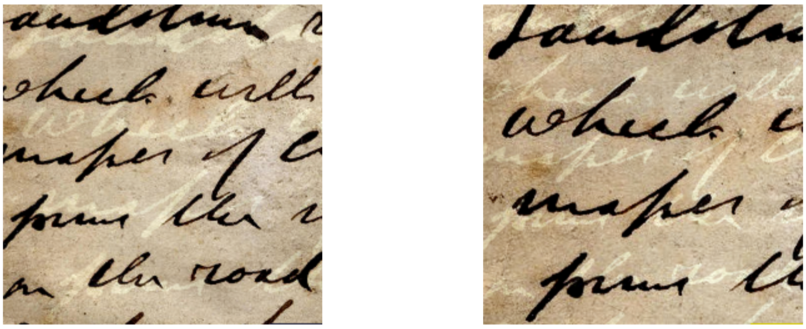

(102.1) recto estimated by MATODS

(102.2) verso estimated by MATODS

Figure 102: Estimates by MATODS

In Table 18 we present the mean square errors with respect to the original documents obtained by means of the above algorithms for the estimate of the recto and the verso of Figure 99.

We consider the ideal images in Figure 107.

Using the above indicated mixture matrices, we synthetically obtain the degraded images in Figure 108.

By applying the algorithms we obtain, as estimates, the results in Figures 109-114.

In Table 19 we present the mean square errors with respect to the original documents obtained by means of the above algorithms for the estimate of the recto and the verso of Figure 107. We consider the ideal images in Figure 115.

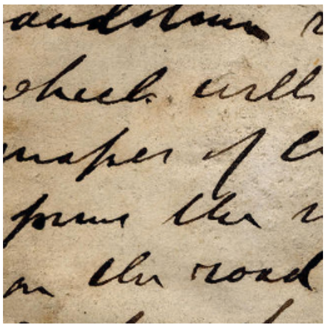

(103.1) recto estimated by FastIca

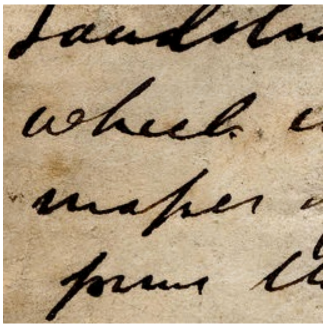

(103.2) verso estimated by FastIca

Figure 103: Estimates by FastIca

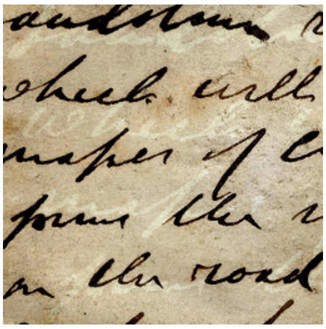

(104.1) recto estimated by Symmetric Whitening

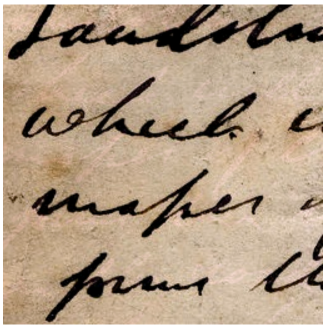

(104.2) verso estimated by Symmetric Whitening

Figure 104: Estimates by Symmetric Whitening

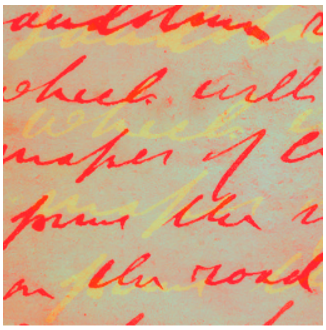

(105.1) recto estimated by Whitening

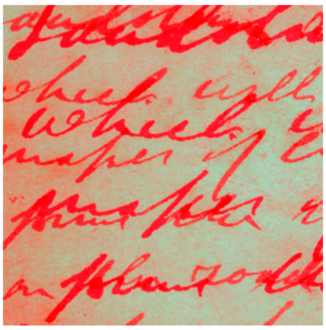

(105.2) verso estimated by Whitening

Figure 105: Estimates by Whitening

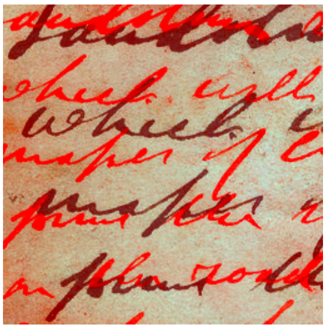

(106.1) recto estimated by PCA

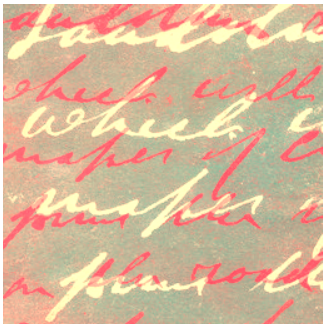

(106.2) verso estimated by PCA

Figure 106: Estimates by PCA

Used Technique	MSE Recto	MSE Verso	MSE of A
ZEODS	0.2423	3.5365	$2.044 \cdot 10^{-5}$
MATODS	35.0330	51.3125	0.0002
FASTICA	4.4079	4.1418	0.0126
Symmetric Whitening	45.8355	117.4545	0.0305
Whitening	$6.7961 \cdot 10^3$	$3.7444 \cdot 10^3$	0.3297
PCA	$1.1179 \cdot 10^4$	$4.1416 \cdot 10^3$	0.3893

Table 18: Errors of the algorithms by using the mixture matrix in (29).

(107.1) original recto

(107.2) original verso

Figure 107: Ideal images

(108.1) degraded recto

(108.2) degraded verso

Figure 108: Degraded images

(109.1) recto estimated by ZEODS

(109.2) verso estimated by ZEODS

Figure 109: Estimates by ZEODS

(110.1) recto estimated by MATODS

(110.2) verso estimated by MATODS

Figure 110: Estimates by MATODS

(111.1) recto estimated by FastIca

(111.2) verso estimated by FastIca

Figure 111: Estimates by FastIca

(112.1) recto estimated by Symmetric Whitening

(112.2) verso estimated by Symmetric Whitening

Figure 112: Estimates by Symmetric Whitening

(113.1) recto estimated by Whitening

(113.2) verso estimated by Whitening

Figure 113: Estimates by Whitening

(114.1) recto estimated by PCA

(114.2) verso estimated by PCA

Figure 114: Estimates by PCA

Used Technique	MSE Recto	MSE Verso	MSE of A
ZEODS	0.4521	1.3566	$1.9913 \cdot 10^{-5}$
MATODS	67.4521	75.6765	0.0007
FASTICA	14.8255	47.8983	0.0429
Symmetric Whitening	221.8945	190.5466	0.0377
Whitening	$1.6127 \cdot 10^3$	421.6936	0.0377
PCA	$3.7456 \cdot 10^3$	$1.3281 \cdot 10^3$	0.3954

Table 19: Errors of the algorithms by using the mixture matrix in (29).

(115.1) original recto

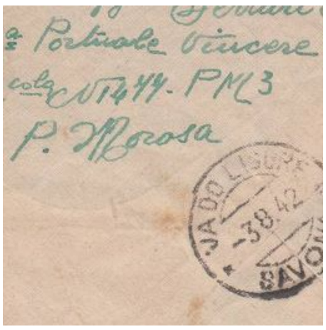

(115.2) original verso

Figure 115: Ideal images

Using the above indicated mixture matrices, we synthetically obtain the degraded images in Figure 116.

(116.1) degraded recto

(116.2) degraded verso

Figure 116: Degraded images

By applying the algorithms we obtain, as estimates, the results in Figures 117-122.

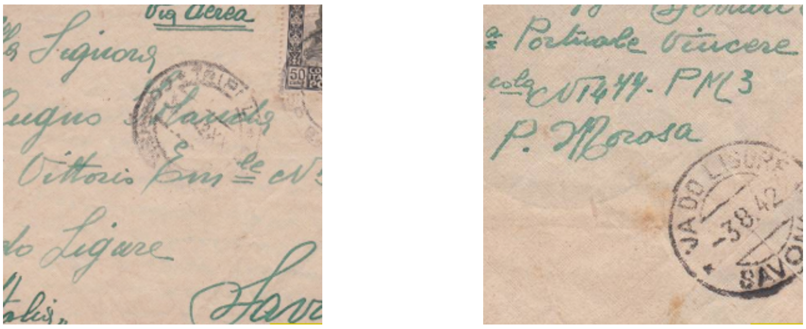

(117.1) recto estimated by ZEODS

(117.2) verso estimated by ZEODS

Figure 117: Estimates by ZEODS

In Table 20 we present the mean square errors with respect to the original documents obtained by means of the above algorithms for the estimate of the recto and the verso of Figure 115.

We consider the ideal images in Figure 123.

Using the above indicated mixture matrices, we synthetically obtain the degraded images in Figure 124.

By applying the algorithms we obtain, as estimates, the results in Figures 125-130.

In Table 21 we present the mean square errors with respect to the original documents obtained by means of the above algorithms for the estimate of the recto and the verso of Figure 123.

(118.1) recto estimated by MATODS

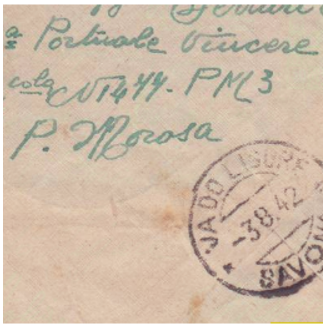

(118.2) verso estimated by MATODS

Figure 118: Estimates by MATODS

(119.1) recto estimated by FastIca

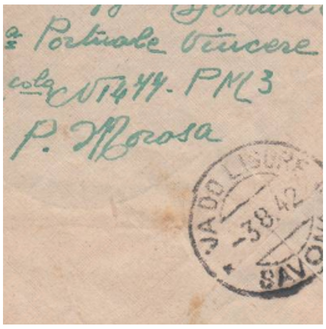

(119.2) verso estimated by FastIca

Figure 119: Estimates by FastIca

(120.1) recto estimated by Symmetric Whitening

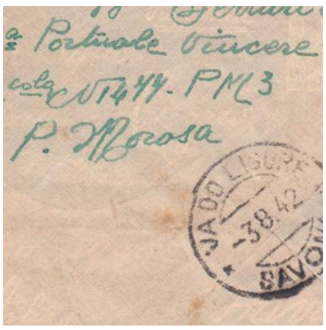

(120.2) verso estimated by Symmetric Whitening

Figure 120: Estimates by Symmetric Whitening

(121.1) recto estimated by Whitening

(121.2) verso estimated by Whitening

Figure 121: Estimates by Whitening

(122.1) recto estimated by PCA

(122.2) verso estimated by PCA

Figure 122: Estimates by PCA

Used Technique	MSE Recto	MSE Verso	MSE of A
ZEODS	0.1486	0.1950	$6.2159 \cdot 10^{-5}$
MATODS	1.9025	2.3132	$2.1564 \cdot 10^{-5}$
FASTICA	0.9037	0.5265	0.0117
Symmetric Whitening	3.8798	12.8583	0.0270
Whitening	$1.7404 \cdot 10^{3}$	833.1407	0.3356
PCA	$2.5707 \cdot 10^{3}$	795.5274	0.3916

Table 20: Errors of the algorithms by using the mixture matrix in (29).

(123.1) original recto

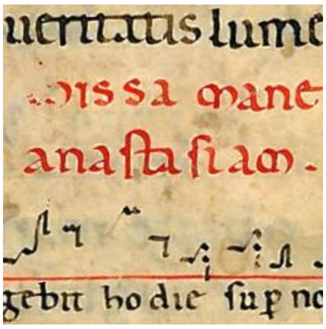

(123.2) original verso

Figure 123: Ideal images

(124.1) degraded recto

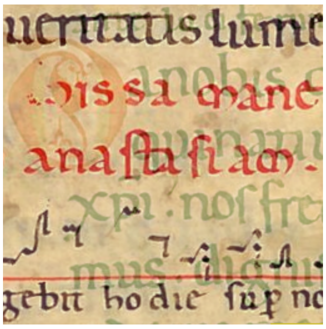

(124.2) degraded verso

Figure 124: Degraded images

(125.1) recto estimated by ZEODS

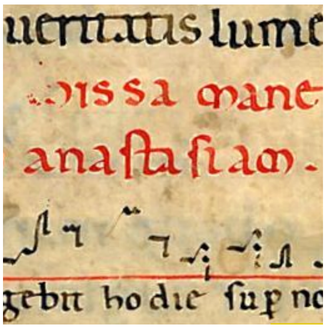

(125.2) verso estimated by ZEODS

Figure 125: Estimates by ZEODS

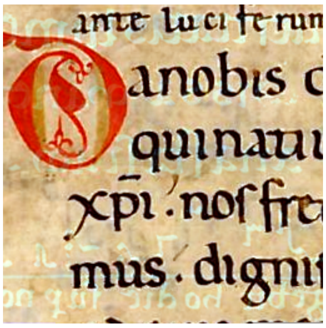

(126.1) recto estimated by MATODS

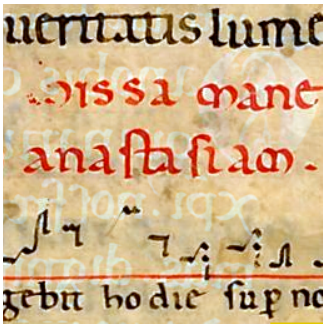

(126.2) verso estimated by MATODS

Figure 126: Estimates by MATODS

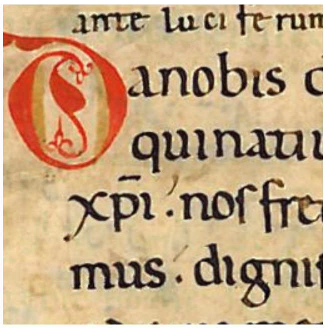

(127.1) recto estimated by FastIca

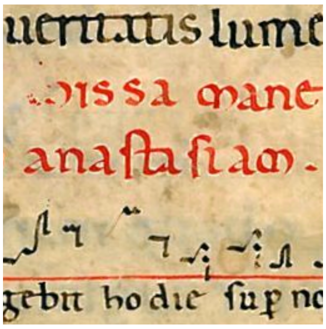

(127.2) verso estimated by FastIca

Figure 127: Estimates by FastIca

(128.1) recto estimated by Symmetric Whitening

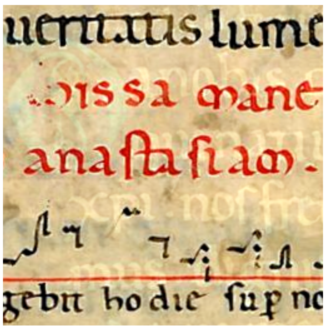

(128.2) verso estimated by Symmetric Whitening

Figure 128: Estimates by Symmetric Whitening

(129.1) recto estimated by Whitening

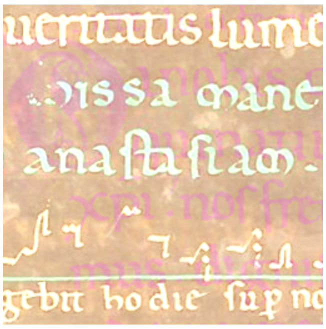

(129.2) verso estimated by Whitening

Figure 129: Estimates by Whitening

(130.1) recto estimated by PCA

(130.2) verso estimated by PCA

Figure 130: Estimates by PCA

Used Technique	MSE Recto	MSE Verso	MSE of A
ZEODS	1.8024	5.2181	$1.012 \cdot 10^{-4}$
MATODS	20.7090	19.3665	0.0001
FASTICA	15.7847	3.3160	0.0223
Symmetric Whitening	7.2817	109.0196	0.0339
Whitening	$1.7703 \cdot 10^4$	$8.5767 \cdot 10^3$	0.0339
PCA	$2.17489 \cdot 10^4$	$5.9721 \cdot 10^3$	0.4655

Table 21: Errors of the algorithms by using the mixture matrix in (29).

As we observe in the previous results, the ZEODS methods, in terms of errors, always obtains better results than the FastIca, PCA, Whitening and Symmetric Whitening algorithms. However, the MATODS algorithm gives results close to those of the proposed algorithm only in the image in Figure 115. To see this, we compare the execution time of the two algorithms in the image in Figure 115.

Used Technique	Time
ZEODS	$0.3510s$
MATODS	$956.3210s$

Table 22: Execution time of the algorithms MATODS and ZEODS by using the mixture matrix in (29) on the image in Figure 115

To see a further demonstration of what we said before, we now make a further test on another image, obtaining similar results by means of both algorithms ZEODS e MATODS.

We consider the ideal images in Figure 131.

(131.1) original recto

(131.2) original verso

Figure 131: Ideal images

Using the above indicated mixture matrices, we synthetically obtain the degraded images in Figure 132.

In Table 23 we present the mean square errors with respect to the original documents obtained by means of the above algorithms for the estimate of the recto and the verso of Figure 131.

By applying the algorithms we obtain, as estimates, the results in Figures 133-134.

As we can note in the results of the previous subsection, the ZEODS method, in terms of errors, always obtains better results than the other algorithms, and is even faster than the MATODS method, as shown in Table 30.

These results given in terms of time are consistent with the previously obtained results.

(132.1) degraded recto

(132.2) degraded verso

Figure 132: Degraded images

Used Technique	MSE Recto	MSE Verso	MSE of A
ZEODS	11.1003	10.4289	$3.7659 \cdot 10^{-5}$
MATODS	4.0124	3.1247	$2.2459 \cdot 10^{-5}$

Table 23: Errors of the algorithms by using the mixture matrix in (29).

(133.1) recto estimated by ZEODS

(133.2) verso estimated by ZEODS

Figure 133: Estimates by ZEODS

(134.1) recto estimated by MATODS

(134.2) verso estimated by MATODS

Figure 134: Estimates by MATODS

Used Technique	Time
ZEODS	$0.3440s$
MATODS	$910.1002s$

Table 24: Execution time of the algorithms MATODS and ZEODS by using the mixture matrix in (29) on the image in Figure 131

4.4 Case 4: Second asymmetric matrix

In the fourth and last case we consider another asymmetric mixture matrix. For every channel R, G and B, the corresponding matrices are

$$A_R = \begin{pmatrix} 0.7 & 0.3 \\ 0.2 & 0.8 \end{pmatrix}, \ A_G = \begin{pmatrix} 0.45 & 0.55 \\ 0.4 & 0.6 \end{pmatrix}, \ A_B = \begin{pmatrix} 0.7 & 0.3 \\ 0.51 & 0.49 \end{pmatrix}. \tag{30}$$

Now we see the behavior of the presented algorithms, regarding both errors and the graphical point of view. We consider the ideal images in Figure 135.

(135.1) original recto

(135.2) original verso

Figure 135: Ideal images

Using the above indicated mixture matrices, we synthetically obtain the degraded images in Figure 136.

By applying the algorithms we obtain, as estimates, the results in Figures 137-142.

In Table 25 we present the mean square errors with respect to the original documents obtained by means of the above algorithms for the estimate of the recto and the verso of Figure 135. We consider the ideal images in Figure 143. Using the above indicated mixture matrices, we synthetically obtain the degraded images in Figure 144.

By applying the algorithms we obtain, as estimates, the results in Figures 145-150.

In Table 26 we present the mean square errors with respect to the original documents obtained by means of the above algorithms for the estimate of the recto and the verso of Figure 143.

(136.1) degraded recto

(136.2) degraded verso

Figure 136: Degraded images

(137.1) recto estimated by ZEODS

(137.2) verso estimated by ZEODS

Figure 137: Estimates by ZEODS

(138.1) recto estimated by MATODS

(138.2) verso estimated by MATODS

Figure 138: Estimates by MATODS

(139.1) recto estimated by FastIca

(139.2) verso estimated by FastIca

Figure 139: Estimates by FastIca

(140.1) recto estimated by Symmetric Whitening

(140.2) verso estimated by Symmetric Whitening

Figure 140: Estimates by Symmetric Whitening

(141.1) recto estimated by Whitening

(141.2) verso estimated by Whitening

Figure 141: Estimates by Whitening

(142.1) recto estimated by PCA

(142.2) verso estimated by PCA

Figure 142: Estimates by PCA

Used Technique	MSE Recto	MSE Verso	MSE of A
ZEODS	3.9507	4.9612	$7.6397 \cdot 10^{-5}$
MATODS	50.1485	41.1745	0.0098
FASTICA	615.3561	346.1334	0.0719
Symmetric Whitening	707.1949	631.6572	0.0520
Whitening	$2.3355 \cdot 10^{3}$	938.1797	0.2227
PCA	$6.5589 \cdot 10^{3}$	$4.1706 \cdot 10^{3}$	0.3401

Table 25: Errors of the algorithms by using the mixture matrix in (30).

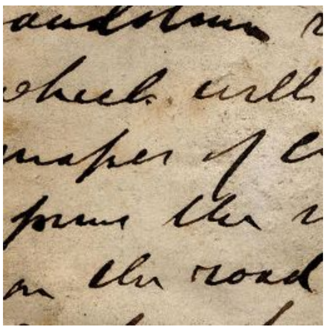

(143.1) original recto

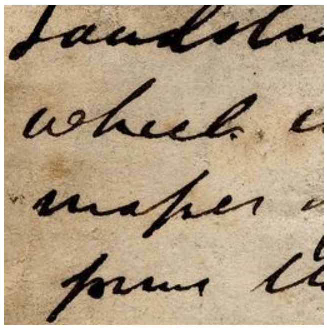

(143.2) original verso

Figure 143: Ideal images

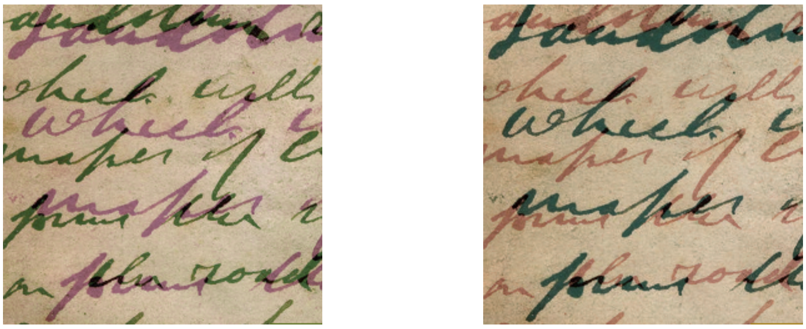

(144.1) degraded recto (144.2) degraded verso

Figure 144: Degraded images

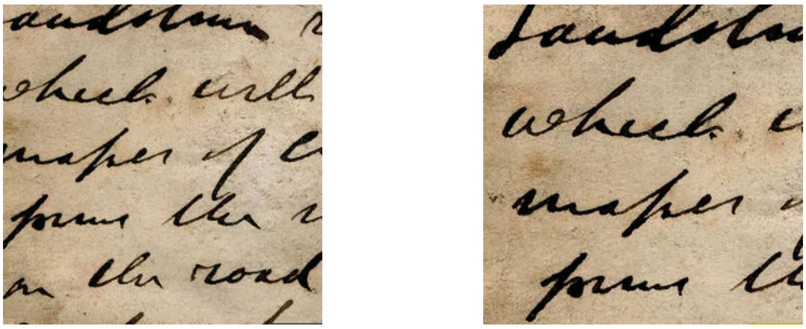

(145.1) recto estimated by ZEODS (145.2) verso estimated by ZEODS

Figure 145: Estimates by ZEODS

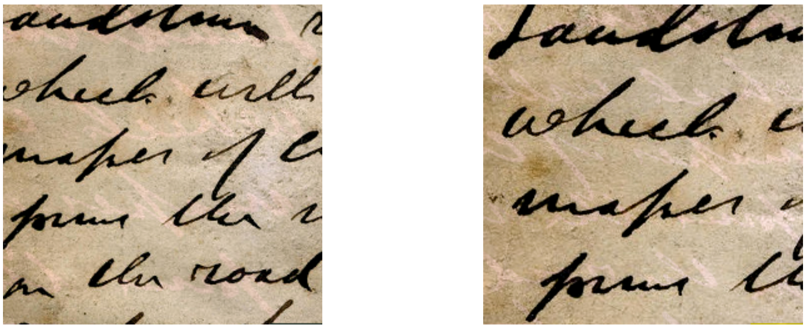

(146.1) recto estimated by MATODS (146.2) verso estimated by MATODS

Figure 146: Estimates by MATODS

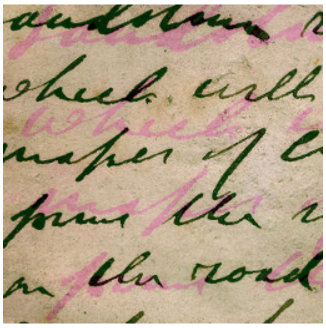

(147.1) recto estimated by FastIca

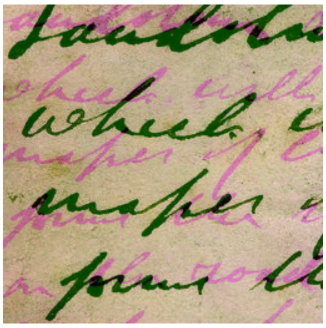

(147.2) verso estimated by FastIca

Figure 147: Estimates by FastIca

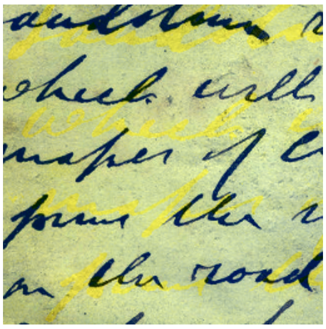

(148.1) recto estimated by Symmetric Whitening

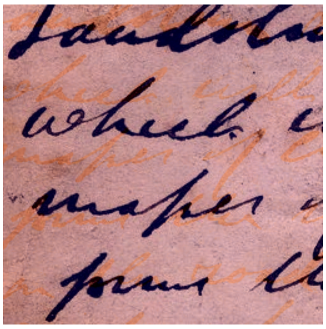

(148.2) verso estimated by Symmetric Whitening

Figure 148: Estimates by Symmetric Whitening

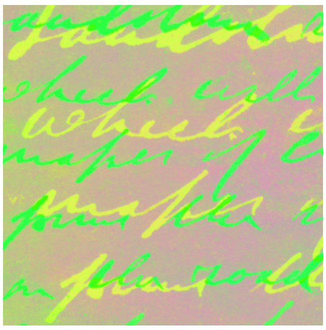

(149.1) recto estimated by Whitening

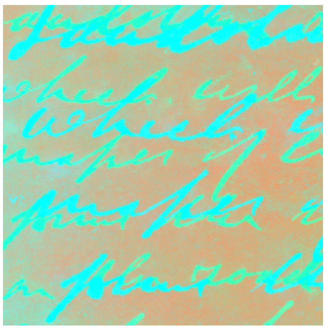

(149.2) verso estimated by Whitening

Figure 149: Estimates by Whitening

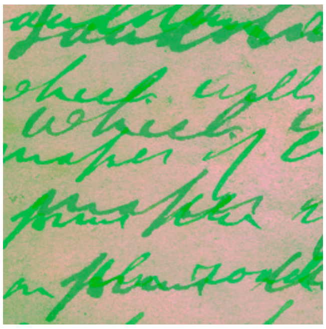

(150.1) recto estimated by PCA

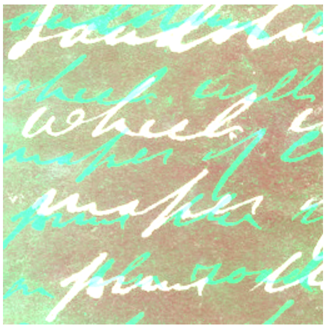

(150.2) verso estimated by PCA

Figure 150: Estimates by PCA

Used Technique	MSE Recto	MSE Verso	MSE of A
ZEODS	1.2642	2.6337	$2.2806 \cdot 10^{-5}$
MATODS	62.2418	85.4395	0.0026
FASTICA	353.226	182.7357	0.0303
Symmetric Whitening	409.8490	495.5137	0.1435
Whitening	$7.7216 \cdot 10^3$	$3.5975 \cdot 10^3$	0.4449
PCA	$1.2810 \cdot 10^4$	$2.5195 \cdot 10^3$	0.4473

Table 26: Errors of the algorithms by using the mixture matrix in (30).

We consider the ideal images in Figure 151.

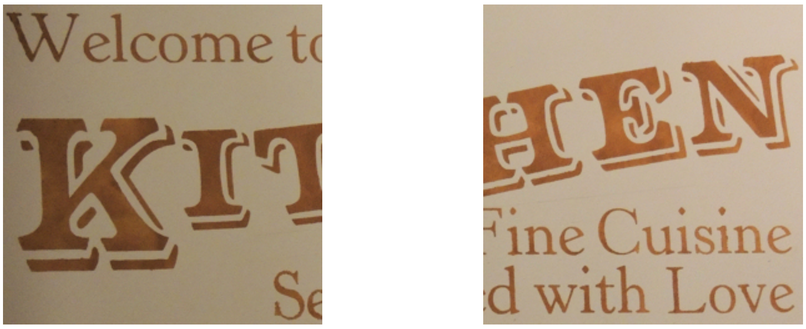

(151.1) original recto (151.2) original verso

Figure 151: Ideal images

Using the above indicated mixture matrices, we synthetically obtain the images in Figure 152. By applying the algorithms we obtain, as estimates, the results in Figures 153-158.

(152.1) degraded recto (152.2) degraded verso

Figure 152: Degraded images

In Table 27 we present the mean square errors with respect to the original documents obtained by means of the above algorithms for the estimate of the recto and the verso of Figure 151. We consider the ideal images in Figure 159.

Using the above indicated mixture matrices, we synthetically obtain the degraded images in Figure 160.

By applying the algorithms we obtain, as estimates, the results in Figures 161-166.

In Table 28 we present the mean square errors with respect to the original documents obtained by means of the above algorithms for the estimate of the recto and the verso of Figure 159.

We consider the following images in Figure 167.

Using the above indicated mixture matrices, we synthetically obtain the degraded images in Figure 168.

(153.1) recto estimated by ZEODS

(153.2) verso estimated by ZEODS

Figure 153: Estimates by ZEODS

(154.1) recto estimated by MATODS

(154.2) verso estimated by MATODS

Figure 154: Estimates by MATODS

(155.1) recto estimated by FastIca

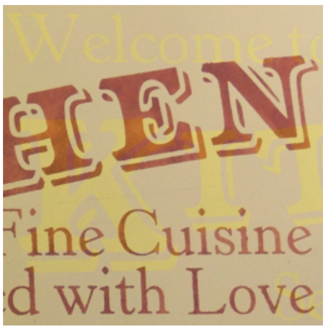

(155.2) verso estimated by FastIca

Figure 155: Estimates by FastIca

(156.1) recto estimated by Symmetric Whitening

(156.2) verso estimated by Symmetric Whitening

Figure 156: Estimates by Symmetric Whitening

(157.1) recto estimated by Whitening

(157.2) verso estimated by Whitening

Figure 157: Estimates by Whitening

(158.1) recto estimated by PCA

(158.2) verso estimated by PCA

Figure 158: Estimates by PCA

Used Technique	MSE Recto	MSE Verso	MSE of A
ZEODS	0.6289	1.3893	$9.6560 \cdot 10^{-6}$
MATODS	12.0247	30.8065	$8.8984 \cdot 10^{-4}$
FASTICA	166.6276	91.2465	0.0386
Symmetric Whitening	352.5150	410.2975	0.0579
Whitening	$1.6118 \cdot 10^{3}$	830.0139	0.3584
PCA	$3.0682 \cdot 10^{3}$	$1.8473 \cdot 10^{3}$	0.3767

Table 27: Errors of the algorithms by using the mixture matrix in (30).

(159.1) original recto

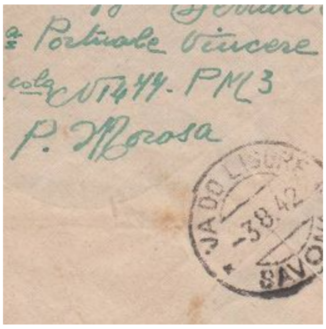

(159.2) original verso

Figure 159: Ideal images

(160.1) degraded recto

(160.2) degraded verso

Figure 160: Degraded images

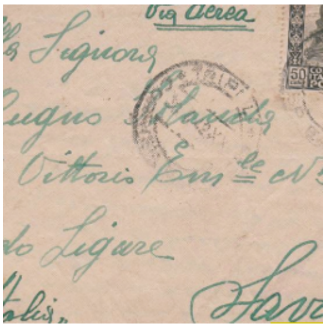

(161.1) recto estimated by ZEODS

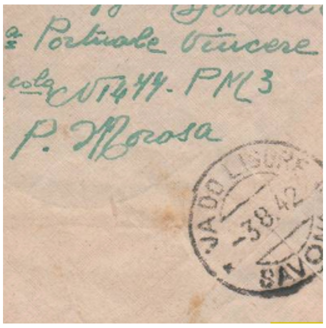

(161.2) verso estimated by ZEODS

Figure 161: Estimates by ZEODS

(162.1) recto estimated by MATODS

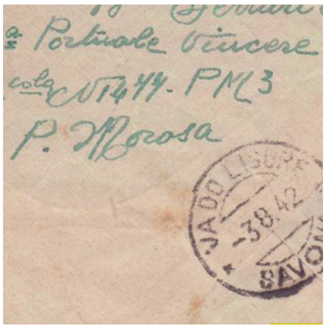

(162.2) verso estimated by MATODS

Figure 162: Estimates by MATODS

(163.1) recto estimated by FastIca

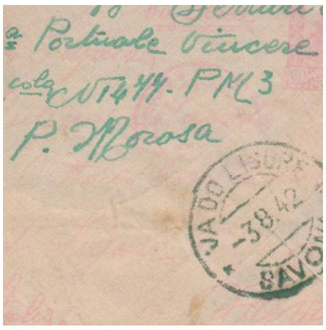

(163.2) verso estimated by FastIca

Figure 163: Estimates by FastIca

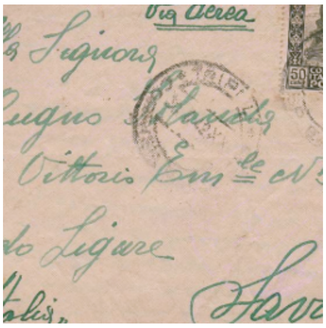

(164.1) recto estimated by Symmetric Whitening

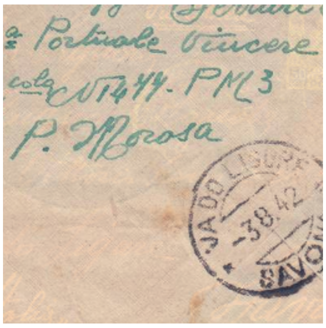

(164.2) verso estimated by Symmetric Whitening

Figure 164: Estimates by Symmetric Whitening

(165.1) recto estimated by Whitening

(165.2) verso estimated by Whitening

Figure 165: Estimates by Whitening

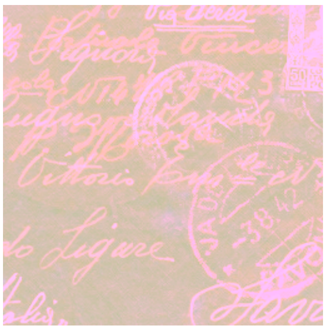

(166.1) recto estimated by PCA

(166.2) verso estimated by PCA

Figure 166: Estimates by PCA

Used Technique	MSE Recto	MSE Verso	MSE of A
ZEODS	0.3876	1.7862	$6.7032 \cdot 10^{-5}$
MATODS	3.1985	5.1475	0.0002
FASTICA	34.7680	15.8122	0.0228
Symmetric Whitening	8.8713	17.2117	0.0458
Whitening	$2.2407 \cdot 10^3$	$1.2194 \cdot 10^3$	0.4580
PCA	$2.8462 \cdot 10^3$	941.9039	0.4180

Table 28: Errors of the algorithms by using the mixture matrix in (30).

(167.1) original recto

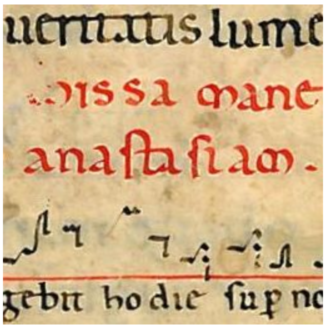

(167.2) original verso

Figure 167: Ideal images

(168.1) degraded recto

(168.2) degraded verso

Figure 168: Degraded images

By applying the algorithms we obtain, as estimates, the results in Figures 169-174.

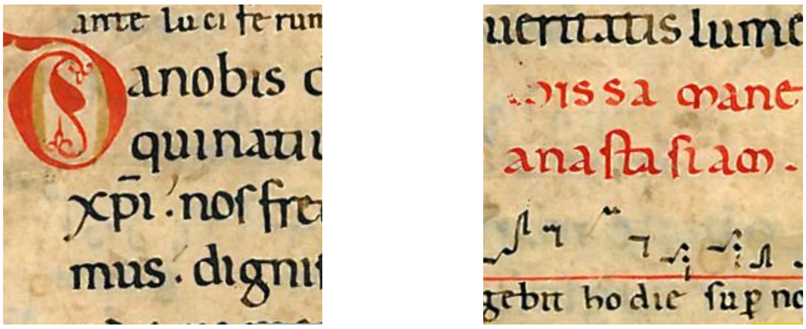

(169.1) recto estimated by ZEODS

(169.2) verso estimated by ZEODS

Figure 169: Estimates by ZEODS

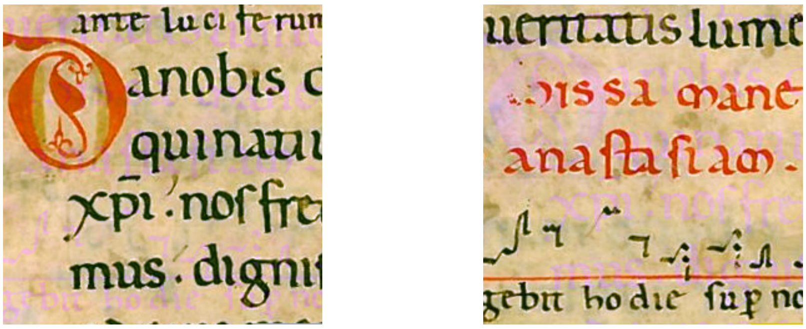

(170.1) recto estimated by MATODS

(170.2) verso estimated by MATODS

Figure 170: Estimates by MATODS

In Table 29 we present the mean square errors with respect to the original documents obtained by means of the above algorithms for the estimate of the recto and the verso of Figure 167.

As we observe in the results of the previous subsection, the ZEODS methods, in terms of errors, always obtains better results than the FastIca, PCA, Whitening and Symmetric Whitening algorithms. However the MATODS algorithm obtains results close to those of the proposed algorithm only in the image in Figure 159. But the execution time of the ZEODS algorithm is much shorter than those of the MATODS algorithm. To see this, we compare the execution time of the two algorithms in the image in Figure 159.

To see a further demonstration of what we said before, we now make a further test on another image, obtaining similar results by means of both algorithms ZEODS e MATODS. We consider the ideal images in Figure 175.

(171.1) recto estimated by FastIca

(171.2) verso estimated by FastIca

Figure 171: Estimates by FastIca

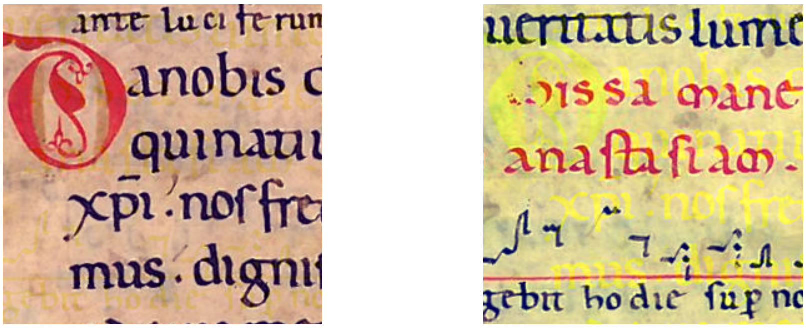

(172.1) recto estimated by Symmetric Whitening

(172.2) verso estimated by Symmetric Whitening

Figure 172: Estimates by Symmetric Whitening

(173.1) recto estimated by Whitening

(173.2) verso estimated by Whitening

Figure 173: Estimates by Whitening

(174.1) recto estimated by PCA

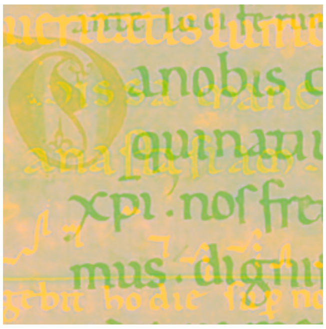

(174.2) verso estimated by PCA

Figure 174: Estimates by PCA

Used Technique	MSE Recto	MSE Verso	MSE of A
ZEODS	3.2977	3.6252	$1.090 \cdot 10^{-4}$
MATODS	35.0124	42.8569	$1.5041 \cdot 10^{-4}$
FASTICA	232.7229	147.4355	0.0304
Symmetric Whitening	235.6894	607.9245	0.1441
Whitening	$1.4669 \cdot 10^4$	$6.6340 \cdot 10^3$	0.5272
PCA	$1.9414 \cdot 10^4$	$3.9348 \cdot 10^3$	0.4795

Table 29: Errors of the algorithms by using the mixture matrix in (30).

Used Technique	Time
ZEODS	$0.3390s$
MATODS	$845.1618s$

Table 30: Execution time of the algorithms MATODS and ZEODS by using the mixture matrix in (30) on the image in Figure 159

(175.1) original recto

(175.2) original verso

Figure 175: Ideal images

Using the above indicated mixture matrices, we synthetically obtain the degraded images in Figure 176.

(176.1) degraded recto

(176.2) degraded verso

Figure 176: Degraded images

In Table 31 we present the mean square errors with respect to the original documents obtained by means of the above algorithms for the estimate of the recto and the verso of Figure 175.

Used Technique	MSE Recto	MSE Verso	MSE of A
ZEODS	8.1003	7.4289	$3.7659 \cdot 10^{-5}$
MATODS	6.0247	5.1247	$2.2459 \cdot 10^{-5}$

Table 31: Errors of the algorithms by using the mixture matrix in (30).

The ZEODS algorithm obtains results very close to the MATODS algorithm. We get, as estimates, the results in Figures 177-178. We analyze the execution time of algorithms. As in

(177.1) recto estimated by ZEODS

(177.2) verso estimated by ZEODS

Figure 177: Estimates by ZEODS

(178.1) recto estimated by MATODS

(178.2) verso estimated by MATODS

Figure 178: Estimates by MATODS

the previous case, we get that the ZEODS method gives results in a much shorter time than the MATODS method, as we can see in Table 30.

Used Technique	Time
ZEODS	$0.3510s$
MATODS	$812.1014s$

Table 32: Execution time of the algorithms MATODS and ZEODS by using the mixture matrix in (29) on the image in Figure 175

These results given in terms of time are consistent with the previously obtained results.

References

[1] A. Boccuto, I. Gerace, and V. Giorgetti, *Minimum Amount of Text Overlapping in Document Separation,* viXra 1805.0284 (2018), pp. 1-91.

[2] A. Boccuto, I. Gerace, and V. Giorgetti, *A Blind Source Separation Technique for Document Restoration,* SIAM J. Imaging Sci., 12 (2) (2019), 1135–1162.

[3] T.-H. Chan, W.-K. Ma, C.-Y. Chi, and Y. Wang, *A Convex Analysis Framework for Blind Separation of Non-Negative Sources,* IEEE Trans. Signal Process., 56 (10) (2008), pp. 5120–5134.

[4] A. Cichocki and S.-I. Amari, *Adaptive Blind Signal and Image Processing,* John Wiley & Sons, Chichester, 2002.

[5] A. Cichocki, R. Zdunek, and S.-I. Amari, *New Algorithms for Non-Negative Matrix Factorization in Applications to Blind Source Separation,* In: Proceedings of the 2006 IEEE International Conference Acoustics, Speech and Signal Processing, Toulouse, France (2006), pp. 1–4.

[6] P. Comon, *Independent Component Analysis, A New Concept?* Signal Processing, 36 (1994), pp. 287–314.

[7] N. Gillis, *Successive Nonnegative Projection Algorithm for Robust Nonnegative Blind Source Separation,* SIAM J. Imaging Sci., 7 (2) (2014), pp. 1420-1450.

[8] N. Gillis, *Sparse and unique nonnegative matrix factorization through data preprocessing,* J. Machine Learning Research, 13 (2012), pp. 3349–3386.

[9] A. Hyvärinen, *Fast and Robust Fixed-Point Algorithms for Independent Component Analysis,* IEEE Trans. Neural Networks, 10 (3) (1999), pp. 626–634.

[10] A. Hyvärinen, *The Fixed-Point Algorithm and Maximum Likelihood Estimation for Independent Component Analysis,* Neural Process. Letters 10, (1) (1999), pp. 1–5.

[11] A. Hyvärinen and E. Oja, *A Fast Fixed-Point Algorithm for Independent Component Analysis,* Neural Computation 9 (7) (1997), pp. 1483–1492.

[12] A. Khaparde, M. Madhavilatha, M. B. L. Manasa, and S. Pradeep Kumar, *FastICA Algorithm for the Separation of Mixed Images,* WSEAS Transactions on Signal Process., 4 (5) (2008), pp. 271–278.

[13] R. K. Malik and K. Solanki, *FastICA Based Blind Source Separation for CT Imaging Under Noise Conditions,* Int. J. Advances in Engineering and Technology, 5 (1) (2012), pp. 47–55.

[14] W. S. B. Ouedraogo, A. Souloumiac, M. Jaidane, and C. Jutten, *Non-Negative Blind Source Separation Algorithm Based on Minimum Aperture Simplicial Cone,* IEEE Transactions on Signal Processing, 62 (2) (2014), pp. 376–389.

[15] A. Tonazzini, I. Gerace, and F. Martinelli, *Multichannel Blind Separation and Deconvolution of Images for Document Analysis,* IEEE Trans. Image Processing, 19 (4) (2010), pp. 912–925.

[16] A. Tonazzini, I. Gerace, and F. Martinelli, *Document Image Restoration and Analysis as Separation of Mixtures of Patterns: From Linear to Nonlinear Models,* in: B.

K. Gunturk and X. Li (Eds.), Image Restoration - Fundamentals and Advances, CRC Press, Taylor & Francis, Boca Raton (2013), pp. 285–310.

[17] A. Tonazzini, E. Salerno, and L. Bedini, *Fast Correction of Bleed-Through Distortion in Greyscale Documents by a Blind Source Separation Technique,* Int. J. Document Analysis 10 (1) (2007), pp. 17–25.

[18] S. Vavasis, *On the Complexity of Nonnegative Matrix Factorization,* SIAM J. Optimization, 20 (3) (2009), pp. 1364–1377.